

# ECoN21

---

Computer Program for Calculating  
Charge Distributions and Bond Valence Sums  
in Crystal Structures

Version 1 Release 8

G. Ilina

*Department of Geology, Mineralogy and Paleontology*

*University of Bucharest*

*Bd. N. Bălcescu, 1, Bucharest*

*e-mail: [gheorghe.ilina@g.unibuc.ro](mailto:gheorghe.ilina@g.unibuc.ro)*

## **LICENSE**

ECoN21 Version 1.8

G. Ilinca

This program is distributed free of charge. Results may be used in publications giving explicit credit to the author, in the form of the following citation:

Ilinca G. (2022) Charge Distribution and Bond Valence Sum Analysis of Sulfosalts. The ECoN21 computer program. *Minerals*, 12, 924. <https://doi.org/10.3390/min12080924>

The software is distributed 'AS IS'. Author makes no other warranties, express or implied.

## Contents

<b>1</b>	<b>Introduction</b>	4
<b>2</b>	<b>The calculation procedure</b>	5
2.1	The charge distribution method	5
2.2	The bond valence sum method	9
2.3	Coordination geometry	11
<b>3</b>	<b>ECaN21 features</b>	13
3.1	Interface and functionality	13
3.2	Listing and saving the results	15
3.3	Interpreting the results	23
<b>4</b>	<b>Calculation settings</b>	25
4.1	The coordination radii	25
4.2	Iteration of weighted average distance	31
4.3	CD iteration methods and convergence criteria	32
4.4	Approximation of the ideal polyhedron	33
<b>5</b>	<b>Input file requirements</b>	37
5.1	Unit cell parameters	37
5.2	Symmetry operators	37
5.3	Atom labels	38
5.4	Atom symbols	38
5.5	Oxidation numbers	39
5.6	Symmetry multiplicities	40
5.7	Fractional coordinates	40
5.8	Occupancies	40
5.9	Troubleshooting CIF issues	41
<b>6</b>	<b>The <i>Ro</i> and <i>B</i> parameters</b>	45
<b>7</b>	<b>Dealing with hydrogen atoms and bonds</b>	47
<b>8</b>	<b>Opposing bond lengths—the Trömel diagram</b>	50
8.1	Definition of 'in plane' and 'out of plane' bond pairs	50
8.2	Bond-length ratio hyperbolae	51
8.3	Step-by-step calculation example	53
8.4	Opposing bond pairs and the coordination number	55
<b>9</b>	<b>The Armbruster—Hummel diagram</b>	57
<b>10</b>	<b>Release notes</b>	58
<b>11</b>	<b>References</b>	61

# 1 Introduction

ECoN21 is a computer program used for the calculation of charge distribution (CD) and concurrently, bond valence sums (BVS) in crystal structures. The program calculates also a wide range of parameters related to the geometry of coordination polyhedra. The input used by ECoN21 is a CIF file containing the crystal structure data.

This is the eighth release of the first version of ECoN21 (see the [release notes](#) at the end of this document). The name of the program derives from **E**ffective **C**oordination **N**umber which is a central concept in the CD analysis. The term was coined by Rudolf Hoppe in 1979, with view to a better characterization of distorted coordination polyhedra with anisotropic distribution of bond strengths. ECoN21 addresses both homoligand and heteroligand crystal structures of normal valence compounds having a large number of atoms, significant isomorphic substitution in mixed sites and distorted coordination polyhedra. Also, the program solves crystal structures with hydrogen bonds. The main intention behind the CD and BVS analysis is to signal wrong fractional coordinates expressed by wrong distances between the central atoms and their ligands, as well as erroneously assigned oxidation numbers and site populations in heterovalent mixed sites, especially when the atom content of such sites is characterized by similar scattering properties and cannot be properly refined in terms of end-member participation.

ECoN21 is a standalone program requiring no installation or additional dynamic libraries. However, it needs to collect the  $R_o$  and  $B$  parameters necessary for the calculation of bond valence sums. The source of these parameters is the *busparm.cif* file which comes packed with the ECoN21 file and which needs to be placed in the same folder as the main executable file.

ECoN21 was written in Delphi and developed in Embarcadero RAD Studio 10.4 CE, both as Windows 32 and 64-bit applications. ECoN21 was tested under 32 and 64-bit Windows 7 and later versions. Until further notice, the current version and future updates of the program can be downloaded from

<https://unibuc.ro/user/gheorghe.ilinca/?profiletab=documents>.

When downloading the program, please write an email to [gheorghe.ilinca@g.unibuc.ro](mailto:gheorghe.ilinca@g.unibuc.ro) or [g.g.ilinca@gmail.com](mailto:g.g.ilinca@gmail.com) so that you can be informed of any updates. Use these email addresses also for pointing out any issues regarding ECoN21's functionality or to require assistance.

All crystal structures in this manual were drafted with VESTA3 (Moma and Izumi, 2011).



## 2 The calculation procedure

### 2.1 The charge distribution method

The second rule of coordination (Pauling, 1929) states that in a stable coordination structure, the charge  $q_A$  of each anion in a coordination polyhedron (CP) tends to compensate *the strength of the electrostatic valence bonds* reaching it from the central cation carrying a charge  $q_X$ :

$$q_A = - \sum_i \left( \frac{q_X}{CN} \right)_i = - \sum_i s_i \quad (1)$$

where  $CN$  is the coordination number and  $s_i$  is the (Pauling's) bond strength. This equation is applicable only to regular polyhedra (e.g., [Figure 1a](#)). Instead, irregular polyhedra (e.g., [Figure 1b](#)) require a *bond length—bond strength* relationship to describe the decrease of the bond strength with increasing bond length.

Both the CD and BVS methods involve power-laws that express this relationship. The differences between the two methods have been extensively described (e.g., Nespolo *et al.*, 1999). In the case of CD, the bonds of a CP are ranked according to their length. Each bond is assigned a *bond weight* that will determine the relative *strength* of that bond. The shortest distance will receive the maximum bond weight and all the other weights will be scaled down following a negative exponential law. This is only possible if all the ligands in a CP are of the same chemical variety. If more chemical species coexist in a CP, the shortest distance of one type can no longer be used for ranking all the other bonds. What may seem too be a 'long' and 'weak' bond for a certain chemical type, could very well be a 'normal' or 'strong' bond for another. Therefore, each chemical type of ligand must have its minimum distance as the scaling parameter.

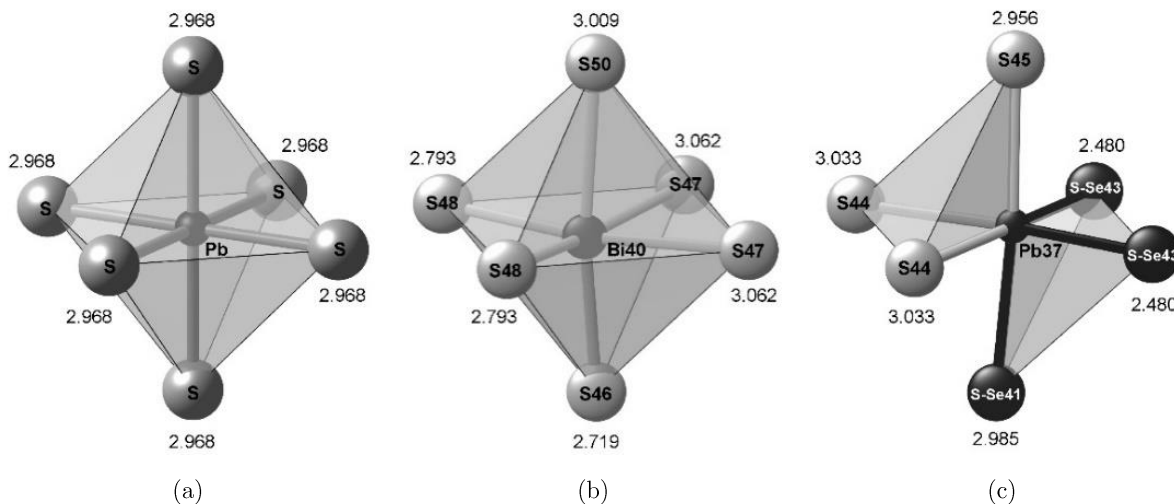


**Figure 1.** Examples of coordination polyhedra: (a) *regular* coordination octahedron in galena (AMCSD 0011372—and reference therein); (b) *irregular homoligand* octahedron around the Bi40 position in cannizzarite (Topa *et al.* 2010); (c) *irregular heteroligand* octahedron around Pb37 in the same crystal structure, with two *homoligand subpolyhedra* defined for pure S and for mixed S-Se ligands. The values near the octahedra's vertices are the bond lengths in ångstroms.

In the most general case, a CP will consist of a central atom surrounded by ligands of different chemical types, situated at different distances, that is, of a *distorted heteroligand* CP. To establish the shortest bond length for each chemical type, the heteroligand polyhedron is divided into several *homoligand subpolyhedra* (HSP) (Nespolo, 2016) ([Figure 1c](#)).

An HSP may contain only one ligand that is implicitly assigned the maximum bond weight, but which may result in an overestimated bond strength at the CP scale. For this reason, the CD calculation for heteroligand CPs must include an iteration procedure which is described later in this section.

The mathematical notation used in this section follows largely the symbolism used by Ferraris (2011) and it aligns with the notation used by VESTA 3. To the extent possible, the terms 'cation' and 'anion' have been avoided throughout the presentation of the calculation procedures. References are made only to the terms 'central atom' and 'ligand'. Thus, the formulas can be used reversely for cation-centered or anion-centered descriptions of the structure, with just the appropriate change of sign and symbol. The main symbols used in the calculation are given below:

- $i$  – the index of ligands in an HSP
- $j$  – the index of HSPs in a CP
- $X$  – the index of crystallographic species of central atoms (or of distinct CPs)
- $A$  – the index of crystallographic species of ligands
- $R_{ij}$  – the distance between the central atom and the  $i^{\text{th}}$  ligand in  $HSP_j$
- $R_{jmin}$  – the minimum distance between the central atom and the ligands in  $HSP_j$
- $\bar{R}_j$  – the weighted average bond distance in  $HSP_j$
- $w_{ij}$  – the bond weight of the  $i^{\text{th}}$  distance in  $HSP_j$
- $ECoN_X$  – the effective coordination number of the CP around central atom  $X$
- $q_X$  – the formal oxidation number of the  $X^{\text{th}}$  crystallographic type of central atom
- $q_A$  – the formal oxidation number of the  $A^{\text{th}}$  crystallographic type of ligand
- $\Delta q_{ij \rightarrow A}$  – the fraction of the formal oxidation number of the central atom shared with the  $i^{\text{th}}$  ligand in  $HSP_j$
- $\Delta q_j$  – the total charge received by the ligands in  $HSP_j$
- $Q_A$  – the total charge of the  $A^{\text{th}}$  crystallographic type of ligand received from all the CPs it belongs to
- $\Delta Q_{ij \leftarrow A}$  – the fraction of the computed charge received by the central atom  $X$  from its  $i^{\text{th}}$  ligand in  $HSP_j$
- $\Delta Q_j$  – the sum of  $\Delta Q_{ij}$  for each  $HSP_j$
- $Q_X$  – the total charge received by the  $X^{\text{th}}$  central atom from the its ligands
- $m_X$  – the multiplicity of the  $X^{\text{th}}$  central atom
- $m_A$  – the multiplicity of the  $A^{\text{th}}$ -type ligand
- $N$  – the order of iteration

For a given CP, a self-consistent *bond length–bond strength relationship* is established through the calculation of the *bond weights*  $w_{ij}$  for each ligand in  $HSP_j$  (Hoppe *et al.*, 1989):

$$w_{ij} = \exp \left[ 1 - \left( \frac{R_{ij}}{\bar{R}_j} \right)^6 \right] \quad (2)$$

where  $\bar{R}_j$  is the *weighted average bond distance*, given by:

$$\bar{R}_j = \frac{\sum_i R_{ij} \exp \left[ 1 - \left( \frac{R_{ij}}{R_{jmin}} \right)^6 \right]}{\sum_i \exp \left[ 1 - \left( \frac{R_{ij}}{R_{jmin}} \right)^6 \right]} \quad (3)$$

$R_{jmin}$  represents the shortest (*i.e.*, the 'strongest') bond in the  $j^{\text{th}}$  HSP. In order to improve the approximation of the weighted mean distance in highly distorted coordination polyhedra, Nespolo *et al.* (2001) suggested an *iterated weighted mean distance*  ${}^N\bar{R}_j$ :

$${}^N\bar{R}_j = \frac{\sum_i R_{ij} \exp \left[ 1 - \left( \frac{R_{ij}}{{}^{N-1}\bar{R}_j} \right)^6 \right]}{\sum_i \exp \left[ 1 - \left( \frac{R_{ij}}{{}^{N-1}\bar{R}_j} \right)^6 \right]} \quad (4)$$

in which  ${}^0\bar{R}_j$  is calculated with Equation (3). The exponent 6 in the equations above, is an empirical parameter introduced by Hoppe in 1979, to approximate the decrease rate of bond weights with increasing bond lengths.

Whenever explicit hydrogen bonds are present in the crystal structure (*i.e.*, hydrogen atoms with listed fractional coordinates and +1 charge), the exponent 6 in Equations (2), (3) and (4) changes to 1.6. This particular value was refined by Nespolo *et al.* (2001) using a large number of structures and it is meant to prevent the quick fall of the hydrogen bond weights with increasing bond distances.

The *effective coordination number* ( $ECoN_X$ ) is calculated for each CP as the sum of all the bond weights:

$$ECoN_X = \sum_j \sum_i w_{ij} \quad (5)$$

$ECoN_X$  is a real number, smaller than or equal to  $CN$ . The parameter  $ECoN_X$  becomes identical with  $CN$  only in the case of regular polyhedra where all  $R_{ij}$  and  $w_{ij}$  values are identical.

The charge of a central atom  $X$ , *i.e.*, the formal oxidation number  $q_X$ , is *distributed* to all the ligands in proportion to the fractional bond strength  $w_{ij}/ECoN_X$ . The *partial charge*  $\Delta q_{ij \rightarrow A}$  (corresponding to Pauling's bond strength) received by a ligand  $A$  from the central atom  $X$ , is given by:

$$\Delta q_{Xij \rightarrow A} = \frac{w_{ij} q_X}{ECoN_X} \frac{m_X}{m_A} \quad (6)$$

The ratio of multiplicities  $m_X/m_A$  ensures that ligands of a certain crystallographic type are counted in the necessary amount and that they receive the right fraction of charge. The oxidation number  $q_X$  is corrected for the site occupancy  $SO$ . In the case of mixed, heterovalent positions, the oxidation number  $q_X$  is calculated as a *weighted average* using the participation  $o_h$  of each of the  $h$  end-members, as the weighting factor:

$$\bar{q}_X = SO \frac{\sum_h q_{Xh} o_h}{\sum_h o_h} \quad (7)$$

The *total charge*  $Q_A$  of the  $A^{\text{th}}$  crystallographic type of ligand is obtained by summation of all  $\Delta q_{ij \rightarrow A}$  received by  $A$  in every CP it belongs to:

$$Q_A = - \sum_X \Delta q_{Xij \rightarrow A} \quad (8)$$

$Q_A$  should be as close as possible to the formal charge of the  $A^{\text{th}}$  ligand, namely,  $q_A$ .

The total charge  $Q_X$  received by the  $X^{\text{th}}$  central atom from its ligands is calculated with:

$$Q_X = \sum_j \sum_i \Delta Q_{ij} = \sum_j \sum_i \Delta q_{Xij \rightarrow A} \frac{q_A}{Q_A} \frac{m_A}{m_X} \quad (9)$$

Thus, any  $q_A/Q_A$  imbalances occurring in the coordination environment of the central atom will influence the value of  $Q_X$  which should be as close as possible to the formal oxidation number  $q_X$ .

If the structure is homoligand, then the calculation stops here. For heteroligand structures, further steps are taken by correcting the partial computed charge  $\Delta Q_{ij}$  received by the central atom  $X$ , with the  $q_X/Q_X$  ratio and by summing the new values for each  $HSP_j$ :

$$\Delta Q_j = \sum_i \Delta Q_{ij} \frac{q_X}{Q_X} \frac{m_X}{m_A} \quad (10)$$

Also, for each  $HSP_j$ , the partial charges are summed up:

$$\Delta q_j = \sum_i \Delta q_{Xij \rightarrow A} \quad (11)$$

The ratio  $\Delta Q_j/\Delta q_j$  is then used to perform the calculation once more, with a new set of  $\Delta q_{ij \rightarrow A}$ :

$${}^N \Delta q_{Xij \rightarrow A} = \frac{\Delta Q_j}{\Delta q_j} {}^{N-1} \Delta q_{Xij \rightarrow A} \quad (12)$$

Alternatively,  $\Delta Q_j$  can be summed up from the  $\Delta Q_{ij \leftarrow X}$  calculated for the ligands of the  $X$  atom when observed in their ligand-centered environment. Thus,  $\Delta Q_j$  will correspond to the  $\Delta Q(ij \rightarrow r) = -\Delta Q(i \rightarrow rs)$  swap in the iteration method described by Nespolo (2016) and used by CHARDI2015. Both iteration methods are included in the ECoN21 program. The calculation can be repeated until convergence is reached by all the CPs in the crystal structure for a given threshold  $T$ , *e.g.*, expressed as the difference between successive  $\Delta Q_j$ :

$${}^N \Delta Q_j - {}^{N-1} \Delta Q_j \leq T \quad (13)$$

Other options for ending the iteration are described in [Section 4.3](#). A graphic representation of the charge distribution is shown in [Figure 2](#).

The calculated charges for the central atom are collected from the last  $Q_X$  sums and the ligand charges, from the last  $Q_A$  values. The overall deviations of  $Q_X$  and of  $Q_A$  from  $q_X$  and  $q_A$  are checked through the calculation of the *mean absolute percentage deviation* (*MAPD*) (Eon and Nespolo, 2015). As an example—for the entire set of  $NX$  central atoms in the asymmetric unit—*MAPD* is calculated as:

$$MAPD_{Q_X} = \frac{100}{NX} \sum_X \left| \frac{q_X - Q_X}{q_X} \right| \quad (14a)$$

To help assessing the under- or overbonding affecting the central atom, the program calculates a similar deviation for the ligands of each CP:

$$MAPD_{L_X} = \frac{100}{CN_X} \sum_A \left| \frac{q_A - Q_A}{q_A} \right|, \quad (14b)$$

where  $A$  counts the crystallographical types of ligands in the CP of atom  $X$ .

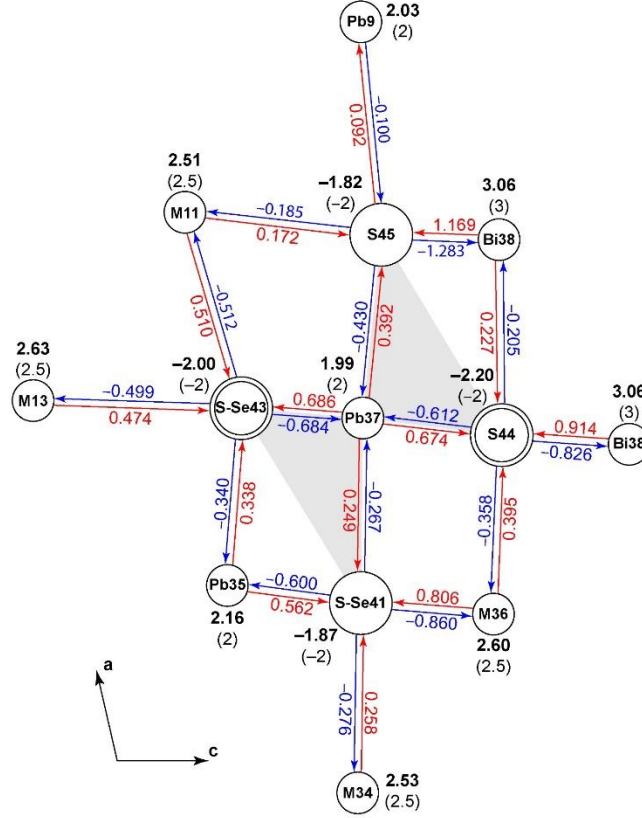


**Figure 2.** The charge distribution around Pb37 in the structure of cannizzarite (Topa et al. [21]). The formal charge of Pb37 ( $q_X = 2$ ) is distributed to the ligands in proportion to the fractional weight of each bond (red arrows diverging from Pb37). The red figures are  $\Delta q_{Xij \rightarrow A}$  values calculated with Equation (6). The total charge  $Q_A$  (e.g., -2.20 for S44) received by each ligand, is the sum of  $\Delta q_{Xij \rightarrow A}$  from all the surrounding central atoms (red arrows converging to each ligand). The total charge  $Q_X = 1.99$  received back by Pb37 from its ligands (blue arrows converging to Pb37) is the sum of  $\Delta Q_{ij}$  values calculated with Equation (9) (blue figures). Ideally,  $Q_X$  and  $Q_A$  should match the formal oxidation numbers  $q_X$  and  $q_A$ , respectively (e.g., +2 for Pb37 and -2 for S44, S45, S-Se41, S-Se43). Figures in bold lettering are the computed charges— $Q_X$  and  $Q_A$ —with the formal oxidation numbers— $q_X$  and  $q_A$ —in parentheses. M11, M13, M34, M36 symbols stand for mixed 0.5Pb-0.5Bi positions ( $q_X = 2.5$ ). Double outlined circles represent pairs of crystallographically similar sulfur atoms overlapping along the  $b$  axis. The shaded areas are projections of the two HSPs defined for the Pb37 CP.

## 2.2 The bond valence sum method

In the case of the BVS method, *partial valences*  $s_{ij}$  (analogues of the Pauling's bond strength) are assigned to each bond of a CP, in correlation with the bond length. The correlation entails empirical exponential curves defined for specific cation-anion pairs and fitted from a large number of structures. Of several equalities describing this correlation, ECoN21 uses Equation (15) (e.g., Brown and Altermatt, 1985):

$$s_{ij} = \exp\left(\frac{R_{oij} - R_{ij}}{B_{ij}}\right), \quad (15)$$

mainly for the abundance of accumulated parameters  $R_{oij}$  and  $B_{ij}$  established for nearly all possible cation-anion bonds (Brown, 2020) and available to ECoN21 via the *bvsparm.cif* file. The term  $R_{oij}$  represents the nominal length for a bond of unit valence, while  $B_{ij}$  denotes the ‘softness factor’, which, in the early works

of Brown and Altermatt (1985) and subsequent collections of bond valence parameters (*e.g.*, Brese and O’Keeffe, 1991) was considered constant, equal to 0.37 Å. In recent years,  $B_{ij}$  for metal-oxygen bonds, has been subjected to ample refinements (*e.g.*, Gagné and Hawthorne, 2015) which established different values for this parameter. The term  $R_{ij}$  represents the  $i^{\text{th}}$  bond length in  $HSP_j$ . Due to its dependence on empirical parameters, the treatment of  $s_{ij}$  in mixed positions may be prone to systematic errors (Bosi, 2014). In this stage of development, the program approximates the  $s_{ij}$  assuming that mixed sites are occupied simultaneously by fractional endmembers.

For mixed positions,  $s_{ij}$  are calculated separately for each endmember and corrected for occupancy:

$$s_{ij} = \frac{\sum_h s_{ijh} o_h}{\sum_h o_h} \quad (16)$$

The significance of  $h$  and  $o_h$  is the same as in [Equation \(7\)](#).

The *bond valence sum* for an entire CP with central site occupancy  $SO \leq 1$  is given by:

$$BVS_X = SO \sum_j \sum_i s_{ij} \quad (17)$$

Ideally, the  $BVS_X$  calculated for a given CP should match the oxidation number  $q_X$  of the central atom. Based on this formal charge and using [Equation \(15\)](#), ECoN21 will calculate the *expected bond distances* for each ligand in the CP:

$$ER_{ij} = R_{oij} - \ln\left(s_{ij} \frac{q_X}{BVS_X}\right) B_{ij} \quad (18)$$

The correction factor  $q_X/BVS_X$  applies to all the bond lengths in a CP and therefore it expands or condenses the entire CP to match  $q_X$ . For mixed positions, both  $R_{oij}$  and  $B_{ij}$  are calculated as weighted averages, using the endmember participations as weighting factors.

The same type of equation as in [\(14a\)](#) is used to obtain the *MAPD* for the entire set of  $BVS_X$  calculated for the  $NX$  central atoms in the asymmetric unit:

$$MAPD_{BVS} = \frac{100}{NX} \sum_X \left| \frac{q_X - BVS}{q_X} \right| \quad (19)$$

The *global instability index* (Brown 2009) is used as a measure of the crystal structure strain: in well balanced and stable structures, the index is smaller than 0.1 v.u.; strained structures yield an index between 0.1 and 0.2 v.u., whereas well-determined structures with the global instability index greater than 0.2 v.u., are rare. For the set of  $NZ$  atoms (cations and anions) in the formula unit, it is calculated as:

$$GII = \sqrt{\frac{1}{NZ} \sum_Z (BVS_Z - q_Z)} \quad (20)$$

The relative charge error is obtained with:

$$EV(\%) = 100 \left| \frac{TX - TA}{TX} \right|, \quad (21)$$

where  $TX$  is the total charge of the cations and  $TA$ , the total charge of the anions, calculated from the structure-derived formula.

### 2.3 Coordination geometry

The CD and BVS calculations are significant only in the context of distorted coordination polyhedra. For this reason, a part of the program is dedicated to the actual geometry of the CP. As shown by Makovicky and Balić-Žunić (1998), two types of distortion may be considered: a) an *internal distortion* given by the displacement of the central atom and by the irregularity of the bond lengths and angles and b) an *external ('volume') distortion* given by the departure of the ligands from the ideal surface of a least-squares fitted (LSF) or 'circumscribed' sphere which approximates their distribution. Both types may be analyzed using quantities related to the centroid of the CP (Makovicky and Balić-Žunić, 1996; Balić-Žunić and Vicković, 1996), that is, to the point against which the variance of the squared distances to the ligands is minimum:

$$\Delta RC = \sum_k \left( RC_k^2 - \frac{\sum_k RC_k^2}{CN_X} \right) \quad (22)$$

where  $RC_k$  represents the  $k^{\text{th}}$  centroid–ligand distance.

The following values are calculated by ECoN21 using the definitions and the procedures published by Makovicky and Balić-Žunić (1996, 1998) and included in the MS-DOS program IVTON (Balić-Žunić and Vicković, 1996):

- the coordinates  $x_o, y_o, z_o$  of the centroid—obtained by expressing Equation (22) in terms of orthogonal coordinates and by solving the linear system formed by the partial derivatives for  $x_o, y_o$  and  $z_o$  which are set equal to zero;
- the components  $I, J, K$  of the vector between the central atom and the centroid—indicating the direction opposite to the lone electron pair of the central atom;
- the displacement  $\Delta$  of the central atom from the centroid;
- the radius  $r_s$  of the LSF 'circumsphere'—represented by the average distance between the centroid and the ligands;
- the volume  $V_s$  of the LSF 'circumsphere';

The quantities in Equations (23–26) were explained in Topa *et al.* (2003).

- the linear eccentricity of the central atom:

$$LEcc = \frac{\Delta}{r_s} \quad (23)$$

- the 'volume-based' eccentricity of the central atom, obtained by comparing the volume of the LSF sphere with the volume of the sphere of radius  $(r_s - \Delta)$ :

$$VEcc = 1 - \left[ \left( 1 - \frac{\Delta}{r_s} \right) \right]^3 \quad (24)$$

- the linear sphericity of the ligand distribution:

$$LSph = 1 - \frac{\sigma_s}{r_s} \quad (25)$$

where  $\sigma_s$  is the standard deviation of the centroid–ligand distances;

- the ‘volume-based’ sphericity of the ligand distribution:

$$VSph = 1 - \frac{3\sigma_s}{r_s} \quad (26)$$

- the volume  $V_r$  of the CP obtained by dividing the CP into tetrahedra delimited by triplets of adjacent vertices and the central atom, and by summation of their volumes;
- the approximation of the ideal polyhedron of maximum volume inscribed in the LSF ‘circumsphere’—established as a function of  $CN$  and number of CP faces;
- the volume  $V_i$  of the ideal polyhedron inscribable in the LSF ‘circumsphere’ and which has the maximum possible volume for that sphere;
- the volume distortion of the CP:

$$v = 1 - \frac{V_r}{V_i} \quad (27)$$

In addition to the parameters derived from the centroid, the following indicators of polyhedral distortion are calculated:

- the deviation of  $ECoN_X$  from  $CNR_X$ :

$$EDEV_X = 1 - \frac{ECoN_X}{CNR_X} \quad (28)$$

where  $CNR_X$  is the number of ligands with bond weights exceeding 0.001 (thus,  $EDEV_X$  does not depend on a  $CN_X$  resulting from an arbitrary setting of the coordination radius).

- the distortion index  $\Delta R(Ba)$  of a coordination polyhedron (Baur 1974):

$$\Delta R(Ba) = \frac{1}{CN_X} \sum_j \sum_i \frac{|R_{ij} - \bar{R}_X|}{\bar{R}_X} \quad (29)$$

where  $\bar{R}_X$  is the average bond length to all the  $CN_X$  ligands in the CP;

- the bond valence-based distortion index  $\Delta R(Br)$  (Brown 2006):

$$\Delta R(Br) = -\frac{B}{CN_X} \sum_j \sum_i \ln\left(\frac{s_{ij}}{\bar{s}_X}\right) \quad (30)$$

where  $\bar{s}_X$  is the average bond valence over all the ligands. In this equation  $\Delta R(Br)$  is independent of the empirical parameter  $R_{oij}$ . As long as the  $B_{ij}$  parameter is constant ( $= B$ ) for all  $R_{ij}$  bonds,  $\Delta R(Br)$  can be used to calculate the polyhedral distortion also for heteroligand polyhedra. As the majority of  $B_{ij}$  parameters are 0.37 Å,  $\Delta R(Br)$  can be considered a good approximation in most situations.

The program also calculates a complete list of bond angles, dihedral angles, interligand bond lengths as well as the distances to the nearest surrounding central atoms within a 5 Å threshold.



## 3 ECoN21 features

### 3.1 Interface and functionality

ECoN21 has a simple and a rather self-explanatory user interface ([Figure 3](#)). The user must open a CIF file, check whether the file was read correctly, run the calculation and get the results, both on screen and in an output file.

The **Open...** button is the first to be pressed after launching ECoN21. This will display a file dialog which filters the CIF files in a chosen folder. After reading the CIF file containing the crystal structure data, the **Space group**, **a**, **b**, **c**, **alpha**, **beta** and **gamma** boxes (Panel 1) will show the information found in the source. The **Atoms** table (Panel 2) will be filled in with the **Atom labels**, **Site populations**, **Oxidation numbers**, symmetry **Multiplicities**, atom coordinates: **X**, **Y**, **Z** and **Occupancies** and should be used to check whether CIF data have been read correctly.

If the CIF file contains negative or larger than 1.0 atom coordinates, these are modified to fit within the unit-cell boundaries. The visual inspection of the data displayed in the table serves as one of the CIF error parsing methods of the program. Missing values, discrepancies between **Space group** and **Multiplicities** or symmetry generated atoms will signal specific errors in the CIF file.

Any mixed (isomorphic) sites are merged and the resulting **Site population** is displayed. If heterovalent mixed sites are encountered, the overall **Oxidation number** is adjusted—in the form of a weighted average—based on each end-member participation ([Equation 7](#)). Adjustments are carried out also for sites with incomplete **Occupancy**.

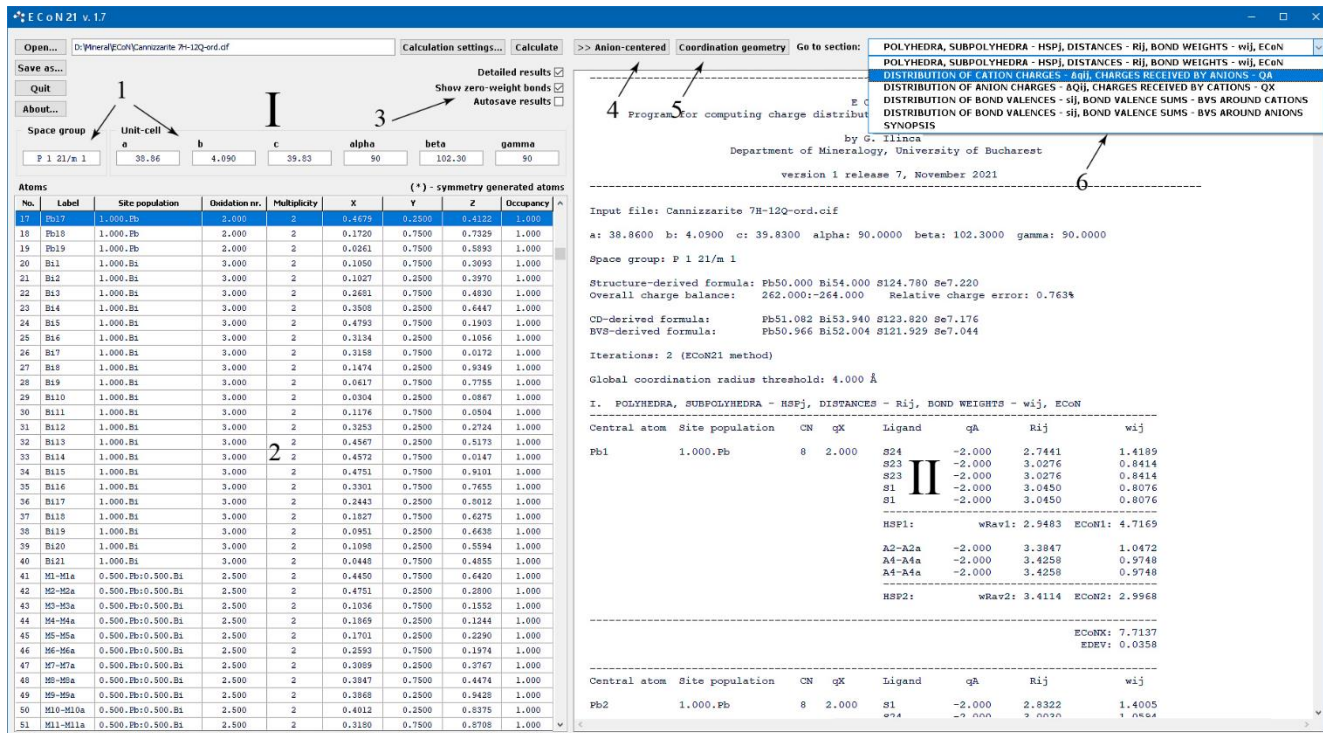
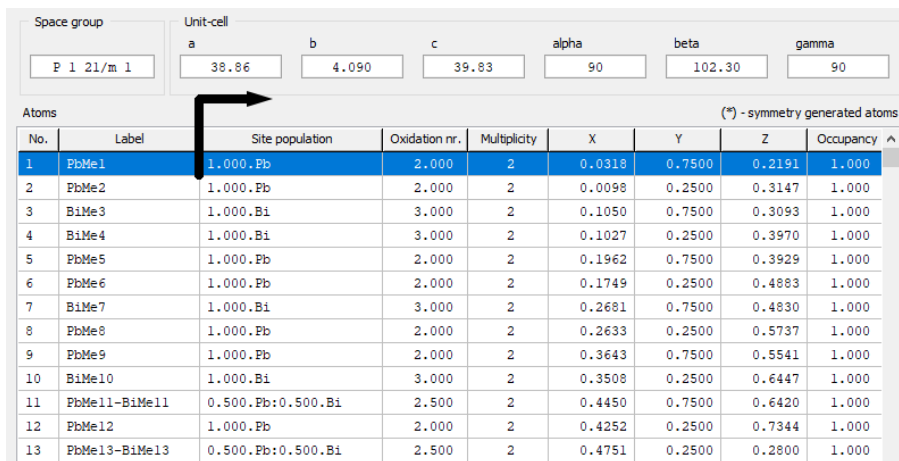


**Figure 3.** The ECoN21's interface: (I) input panel; (II) results panel; (1) space group and unit-cell parameters panels; (2) atoms table; (3) visualization and save options; (4) switch to anion-centered view and back; (5) button for visualization of coordination geometry; (6) navigation aid for long outputs.

The lower part of the **Atoms** table contains the atoms generated by symmetry. All generated atoms are marked with an asterisk sign (\*). The table may be scrolled up and down using the vertical control or with the mouse wheel. In order to reveal the content that does not fit into the table cell width, columns can be resized from their header at runtime ([Figure 4](#)). A mouse double-click over the table restores the default column width.



Space group: **P 1 21/m 1**

Unit-cell parameters:

a	b	c	alpha	beta	gamma
38.86	4.090	39.83	90	102.30	90

Atoms table header: (\*) - symmetry generated atoms

No.	Label	Site population	Oxidation nr.	Multiplicity	X	Y	Z	Occupancy
1	PbMe1	1.000.Pb	2.000	2	0.0318	0.7500	0.2191	1.000
2	PbMe2	1.000.Pb	2.000	2	0.0098	0.2500	0.3147	1.000
3	BiMe3	1.000.Bi	3.000	2	0.1050	0.7500	0.3093	1.000
4	BiMe4	1.000.Bi	3.000	2	0.1027	0.2500	0.3970	1.000
5	PbMe5	1.000.Pb	2.000	2	0.1962	0.7500	0.3929	1.000
6	PbMe6	1.000.Pb	2.000	2	0.1749	0.2500	0.4883	1.000
7	BiMe7	1.000.Bi	3.000	2	0.2681	0.7500	0.4830	1.000
8	PbMe8	1.000.Pb	2.000	2	0.2633	0.2500	0.5737	1.000
9	PbMe9	1.000.Pb	2.000	2	0.3643	0.7500	0.5541	1.000
10	BiMe10	1.000.Bi	3.000	2	0.3508	0.2500	0.6447	1.000
11	PbMe11-BiMe11	0.500.Pb:0.500.Bi	2.500	2	0.4450	0.7500	0.6420	1.000
12	PbMe12	1.000.Pb	2.000	2	0.4252	0.2500	0.7344	1.000
13	PbMe13-BiMe13	0.500.Pb:0.500.Bi	2.500	2	0.4751	0.2500	0.2800	1.000

**Figure 4.** The panel 1 (in [Figure 3](#)) displaying the space group and the unit-cell parameters read from the CIF file and the panel 2 containing the **Atoms** table. The table header can be used to widen the column in order to see the cell content that could not fit in the default cell width.

The **Calculate** button will then be enabled and waiting to be pressed. The results of the calculation are displayed in the right side pane of the main window.

Prior to running the calculation, the user may change the distance range within which the program will search for ligands. This is achieved by pushing the **Calculation settings...** button which opens a dialog box with options for setting bond length limits. Details and examples on how to work with the [Calculation settings](#) dialog are given in [Section 4](#) of this manual.

The visualization options area of panel I contains the following controls:

**Detailed results** ☒ The check box toggles the results view between a summary table and a detailed listing

**Show zero-weight bonds** ☒ Allows the exclusion of long distances with zero-weight from the detailed output listing. However, this does not modify the *CN* established with the coordination thresholds in the [Calculation settings](#) dialog (for *de facto* elimination of zero-weight bonds from the coordination polyhedra, see [Section 4.1](#) of this manual).

**Autosave results** ☒ When checked **on**, the control will trigger the automatic saving of whatever is displayed in the results pane. The saved files will keep the original CIF file name, plus a series of suffixes which are suggestive for a particular visualization of the results. When checked **off**, the **Save as...** button becomes active and the user may choose which type of results to save: detailed or summary CD-BVS results in text or Comma Separated Values (.csv) format, or listings of **Coordination geometry** parameters. The name of the saved file can also be modified and accidental overwriting of files prevented.

## 3.2 Listing and saving the results

Each output listing starts with a header showing the name of the input file, the **unit-cell parameters**, the **space group**, the **structure-derived formula**, the **overall charge balance** and the **relative charge error** (Equation 21). For a first-sight comparison, also the **CD-** and the **BVS-derived formulas** are given. The iteration method used and the coordination radius are also shown in this header:

```
-----
Input file: Cannizzarite 7H-12Q.CIF

a: 38.8600  b: 4.0900  c: 39.8300  alpha: 90.0000  beta: 102.3000  gamma: 90.0000

Space group: P 1 21/m 1

Structure-derived formula: Pb50.000 Bi54.000 S124.780 Se7.220
Overall charge balance:   262.000:-264.000   Relative charge error: 0.763%

CD-derived formula:       Pb51.154 Bi53.899 S123.772 Se7.222
BVS-derived formula:      Pb50.966 Bi52.004 S121.929 Se7.044

Iterations: 2 (ECoN21 method)

Global coordination radius threshold: 4.000 Å
-----
```

The default view of the calculation output is a summary of the main parameters of interest, allowing for a quick inspection of the quality of the results (fragment):

```
-----
CN      - Coordination number
ECoN    - Effective coordination number
EDEV    - Deviation of ECoN from CN
QX      - Charge received by cations
qX      - Oxidation number of cations
BVS     - Bond valence sum
QA      - Charge received by anions
qA      - Oxidation number of anions
MAPDL   - Mean absolute percentage deviation of ligands QA
MAPD    - Mean absolute percentage deviation of QX, QA and BVS
-----
```

Cation	CN	ECoN	EDEV	qX	QX	qX/QX	MAPDL	BVS
Pb1	8	7.714	0.036	2.000	2.158	0.927	5.042	1.953
Pb2	8	7.533	0.058	2.000	2.081	0.961	3.935	1.817
Bi3	6	5.819	0.030	3.000	3.126	0.960	4.607	2.780
Bi4	6	5.790	0.035	3.000	3.010	0.997	2.236	2.848
Pb5	7	6.848	0.022	2.000	2.126	0.941	5.411	2.039
. . . . .								
Bi49	6	5.282	0.120	3.000	2.902	1.034	7.330	2.927
Bi50	6	5.766	0.039	3.000	2.797	1.073	6.987	3.092
Pb51	6	5.931	0.012	2.000	1.959	1.021	6.198	2.250
Bi52	6	5.484	0.086	3.000	2.908	1.032	3.579	2.696
MAPD: 3.70%								6.29%

```
-----
```

Anion	qA	QA	qA/QA	BVS
S1	-2.000	-1.816	1.101	1.977
S2	-2.000	-2.061	0.970	2.021
S3	-2.000	-1.935	1.034	2.022
S4	-2.000	-1.967	1.017	2.012
S5	-2.000	-1.788	1.119	1.968
. . . . .				
S63	-2.000	-2.096	0.954	2.089
S64	-2.000	-1.922	1.041	2.007
S65	-2.000	-2.099	0.953	1.995
S66	-2.000	-2.019	0.990	1.934
MAPD: 6.05%				4.56%

```
-----
```

The first displayed results are for the cation-centered description of the crystal structure. The >> Anion-centered button allows to switch the view for the anion-centered description. Once the anion-centered listing is visible, the switch button changes to >> Cation-centered allowing the return to the first output view.

The detailed results of the calculation include several sections. Examples are given further on, in the form of actual excerpts from ECoN21 output listing. Below is the typical layout for a heteroligand polyhedron containing two homoligand subpolyhedra (see [Section 2.1](#) and [Figure 1c](#)): HSP1 and HSP2, each with its own weighted average bond length ( $wRav$ ) and  $ECoN_X$ .  $CN$  is the coordination number,  $q_X$  is the formal oxidation number of the central atom,  $q_A$  is the formal oxidation number of a ligand,  $R_{ij}$  is the bond length and  $w_{ij}$  is the bond weight calculated with [Equation \(2\)](#).

The deviation  $EDEV_X$  of  $ECoN_X$  from  $CNR_X$  ([Equation 28](#)) also appears at the bottom of each table.

POLYHEDRA, SUBPOLYHEDRA - HSPj, DISTANCES - Rij, BOND WEIGHTS - wij, ECoN										
Central atom	Site population	CN	qX	Ligand	qA	Rij	wij			
Pb1	1.000.Pb	8	2.000	S24	-2.000	2.7441	1.4189			
				S23	-2.000	3.0276	0.8414			
				S23	-2.000	3.0276	0.8414			
				S1	-2.000	3.0450	0.8076			
				S1	-2.000	3.0450	0.8076			
				HSP1:		wRav1: 2.9483	ECoN1: 4.7169			
				S27-Se27	-2.000	3.3847	1.0472			
				S30-Se30	-2.000	3.4258	0.9748			
				S30-Se30	-2.000	3.4258	0.9748			
				HSP2:		wRav2: 3.4114	ECoN2: 2.9968			
										ECoNX: 7.7137
										EDEV: 0.0358

The next table shows the results for a homoligand coordination polyhedron (single HPS):

Central atom	Site population	CN	qX	Ligand	qA	Rij	wij
Bi4	1.000.Bi	6	3.000	S3	-2.000	2.6843	1.3313
				S4	-2.000	2.8418	0.9950
				S4	-2.000	2.8418	0.9950
				S2	-2.000	2.8951	0.8839
				S2	-2.000	2.8951	0.8839
				S66	-2.000	2.9872	0.7006
						wRav: 2.8395	ECoNX: 5.7897
						EDEV: 0.0350	

This is the right place to observe if ligands included in the CP, following a chosen coordination radius threshold, bear zero or close to zero-weight bonds and decide whether such ligands should actually be included in the CP (example for a 4 Å global coordination radius):

Central atom	Site population	CN	qX	Ligand	qA	Rij	wij
As35	1.000.As	8	3.000	S94	-2.000	2.2413	1.2851
				S41	-2.000	2.3050	1.1204
				S3	-2.000	2.5806	0.4746
				S60	-2.000	2.7778	0.1800
				S108	-2.000	3.1162	0.0121
				S82	-2.000	3.5497	0.0000
				S130	-2.120	3.8284	0.0000
				S37	-2.000	3.8992	0.0000
wRav: 2.3518						ECoNX: 3.0723	
EDEV: 0.3855							

The next section contains the results of  $\Delta q_{ij \rightarrow A}$  calculation ([Equation 6](#)) and the computed charges  $Q_A$  for ligands ([Equation 8](#)). In this example,  $Q_A$  for S27–Se27 is the sum (with changed sign) of  $\Delta q_{ij \rightarrow A}$  over all the coordination polyhedra this anion belongs to. A slight negative charge excess is apparent.

DISTRIBUTION OF CATION CHARGES - Δq <sub>ij</sub> AND CHARGES RECEIVED BY ANIONS - Q <sub>A</sub>							
Anion	q <sub>A</sub>	m <sub>A</sub>	Cation	Site population	q <sub>X</sub>	m <sub>X</sub>	Δq <sub>ij</sub>
S27-Se27	-2.000	2	BiMe26	1.000.Bi	3.000	2	0.5339
			BiMe26	1.000.Bi	3.000	2	0.5339
			PbMe28-BiMe28	0.500.Pb:0.500.Bi	2.500	2	0.4753
			PbMe23	1.000.Pb	2.000	2	0.2895
			PbMe1	1.000.Pb	2.000	2	0.2688
-----							
Q <sub>A</sub> (S27-Se27): -2.1015							

Using [Equation \(9\)](#), the partial ( $\Delta Q_{ij \leftarrow A}$ ) and the total charges received by the cations ( $Q_X$ ) are calculated:

DISTRIBUTION OF ANION CHARGES - ΔQ <sub>ij</sub> AND CHARGES RECEIVED BY CATIONS - Q <sub>X</sub>									
Cation	q <sub>X</sub>	m <sub>X</sub>	Anion	Site population	q <sub>A</sub>	m <sub>A</sub>	Δq <sub>ij</sub>	q <sub>A</sub> /Q <sub>A</sub>	ΔQ <sub>ij</sub>
Pb19	2.000	2	S18	1.000.S	-2.000	2	0.3603	0.9879	-0.3560
			S19	1.000.S	-2.000	2	0.2906	1.1323	-0.3290
			S19	1.000.S	-2.000	2	0.2906	1.1323	-0.3290
			S17	1.000.S	-2.000	2	0.1992	0.9789	-0.1950
			S17	1.000.S	-2.000	2	0.1992	0.9789	-0.1950
			S31-Se31	0.770.S:0.230.Se	-2.000	2	0.2946	0.9134	-0.2691
			S31-Se31	0.770.S:0.230.Se	-2.000	2	0.2946	0.9134	-0.2691
			S28-Se28	0.690.S:0.310.Se	-2.000	2	0.0708	0.9977	-0.0707
							MAPDL: 4.9535		

A fourth section of the output listing deals with the bond valence sums of each cation- and anion-centered polyhedron. The bond strengths  $s_{ij}$  are calculated using [Equation \(15\)](#) and summed up to give the  $BVS_X$  or  $BVS_A$  for the entire polyhedron.  $ER_{ij}$  is the expected bond distance calculated with [Equation \(18\)](#) for a theoretical  $BVS_X$  or  $BVS_A$ . Each table ends with the value of Brown distortion index calculated with [Equation \(30\)](#).  $BVS_{X(A)}$  is expressed in valence units and it is always positive. It may be compared directly to  $q_X$ , but also to  $-q_A$ .

DISTRIBUTION OF BOND VALENCES - $s_{ij}$ AND THE BOND VALENCE SUMS - BVS AROUND CATIONS						
Central atom	Site population	qX	Ligand	R <sub>ij</sub>	$s_{ij}$	ER <sub>ij</sub>
Pb11-Bi11	0.500.Pb:0.500.Bi	2.500	S10	2.7692	0.5616	2.7350
			S11	2.9006	0.3937	2.8664
			S11	2.9006	0.3937	2.8664
			S9	2.9540	0.3409	2.9197
			S9	2.9540	0.3409	2.9197
			S45	3.1872	0.1815	3.1529
			S43-Se43	3.8696	0.0341	3.8315
			S43-Se43	3.8696	0.0341	3.8315
Distortion index (Brown): 0.1396			BVS (Pb11-Bi11): 2.2805			

DISTRIBUTION OF BOND VALENCES - $s_{ij}$ AND THE BOND VALENCE SUMS - BVS AROUND ANIONS						
Central atom	Site population	qA	Ligand	R <sub>ij</sub>	$s_{ij}$	ER <sub>ij</sub>
S9	1.000.S	-2.000	BiMe10	2.6478	0.8103	2.6744
			PbMe11-BiMe11	2.9540	0.3409	2.9803
			PbMe11-BiMe11	2.9540	0.3409	2.9803
			PbMe9	2.9529	0.3285	2.9795
			PbMe9	2.9529	0.3285	2.9795
-----						
Distortion index (Brown): 0.0272				BVS (S9): 2.1492		

The final section displays a table similar to the one described for the summary results, but including the **site populations** and the **bonding atoms**. The **bonding atoms** are ordered according to their charge contribution to the central atom. Ligands with charge contributions below 0.01 are listed between square brackets—[ ], whereas ligands contributing with less than 0.1 but with more than 0.01 appear between parentheses—( ). The section shows the global *MAPDs* for  $Q_X$ ,  $Q_A$  and *BVS*, as well as the global instability index calculated with Equation (20):

#### SYNOPSIS (fragment)

Cation	Site population	Bonding atoms	CN	ECnN	EDEV	qX	QX	qX/QX	MAPDL	BVS
Pb1	1.000.Pb	S24,S23,S23,S1,S1,S-Se27,S-Se30,S-Se30	8	7.714	0.036	2.000	2.158	0.927	5.042	1.953
Pb2	1.000.Pb	S1,S24,S24,S2,S2,S64,S64,S-Se61	8	7.533	0.058	2.000	2.081	0.961	3.935	1.817
Bi3	1.000.Bi	S2,S1,S1,S3,S3,S-Se33	6	5.819	0.030	3.000	3.126	0.960	4.607	2.780
Bi4	1.000.Bi	S3,S4,S4,S2,S2,S66	6	5.790	0.035	3.000	3.010	0.997	2.236	2.848
Pb5	1.000.Pb	S4,S5,S5,S3,S3,S-Se36,S-Se36	7	6.848	0.022	2.000	2.126	0.941	5.411	2.039
Pb6	1.000.Pb	S5,S6,S6,S4,S4,(S63),(S63),S-Se60	8	7.088	0.114	2.000	2.063	0.970	4.621	1.794
Bi7	1.000.Bi	S6,S7,S7,S5,S5,S-Se39	6	5.833	0.028	3.000	3.240	0.926	6.629	3.048
Pb8	1.000.Pb	S7,S8,S8,S6,S6,(S57),(S57),S-Se60	8	6.590	0.176	2.000	2.028	0.986	7.432	1.937
Pb9	1.000.Pb	S8,S9,S9,S7,S7,S42,S42,S45	8	6.996	0.126	2.000	2.034	0.983	7.336	1.945
Bi10	1.000.Bi	S9,S8,S8,S10,S10,S54	6	5.361	0.106	3.000	2.864	1.047	4.552	2.765
Pb-Bi11	0.500.Pb:0.500.Bi	S10,S11,S11,S9,S9,S45,S-Se43,S-Se43	8	7.665	0.042	2.500	2.514	0.994	4.979	2.281
Pb12	1.000.Pb	S11,S10,S10,S12,S12,S51,S51,(S54)	8	6.883	0.140	2.000	2.013	0.993	3.861	1.921
Pb-Bi13	0.500.Pb:0.500.Bi	S12,S11,S11,S13,S13,S40,S-Se43,S-Se43	8	7.495	0.063	2.500	2.630	0.951	5.770	2.381
Bi14	1.000.Bi	S13,S14,S14,S12,S12,S48	6	5.776	0.037	3.000	3.044	0.986	3.101	2.945
Pb47	1.000.Pb	S56,S58,S58,S59,S59,S61-S61	6	5.959	0.007	2.000	2.047	0.977	6.270	2.053
Bi48	1.000.Bi	S57,S62,S59,S59,S60-S60,S60-S60	6	5.897	0.017	3.000	2.952	1.016	10.387	2.941
Bi49	1.000.Bi	S64,S62,S62,S59,S61-S61,S61-S61	6	5.282	0.120	3.000	2.902	1.034	7.330	2.927
Bi50	1.000.Bi	S63,S63,S62,S62,S65,S60-S60	6	5.766	0.039	3.000	2.797	1.073	6.987	3.092
Pb51	1.000.Pb	S64,S64,S66,S65,S65,S62	6	5.931	0.012	2.000	1.959	1.021	6.198	2.250
Bi52	1.000.Bi	S66,S66,S63,S65,S65,S65	6	5.484	0.086	3.000	2.908	1.032	3.579	2.696

MAPD: 3.70%

6.29%

Anion	Site population	qA	QA	qA/QA	BVS
S1	1.000.S	-2.000	-1.816	1.101	1.977
S2	1.000.S	-2.000	-2.061	0.970	2.021
S3	1.000.S	-2.000	-1.935	1.034	2.022
S4	1.000.S	-2.000	-1.967	1.017	2.012
S5	1.000.S	-2.000	-1.788	1.119	1.968
S6	1.000.S	-2.000	-1.925	1.039	2.066
S7	1.000.S	-2.000	-1.818	1.100	1.856
S8	1.000.S	-2.000	-2.149	0.931	2.067
S9	1.000.S	-2.000	-2.077	0.963	2.149
S10	1.000.S	-2.000	-2.077	0.963	2.043
S11	1.000.S	-2.000	-1.863	1.073	2.049
S12	1.000.S	-2.000	-1.936	1.033	1.976
S13	1.000.S	-2.000	-1.884	1.061	2.084
S14	1.000.S	-2.000	-2.051	0.975	2.038
S-Se61	0.890.S:0.110.Se	-2.000	-2.015	0.993	1.792
S62	1.000.S	-2.000	-2.319	0.863	2.005
S63	1.000.S	-2.000	-2.096	0.954	2.089
S64	1.000.S	-2.000	-1.922	1.041	2.007
S65	1.000.S	-2.000	-2.099	0.953	1.995
S66	1.000.S	-2.000	-2.019	0.990	1.934

MAPD: 6.05%

4.56%

Global Instability Index: 0.15 v.u.

Elapsed time: 0.367 seconds

For very long detailed outputs, the **Go to section** drop down list located above the results pane helps to navigate rapidly between various results sections (Figure 5). The drop down list is enabled only when the detailed results are displayed.

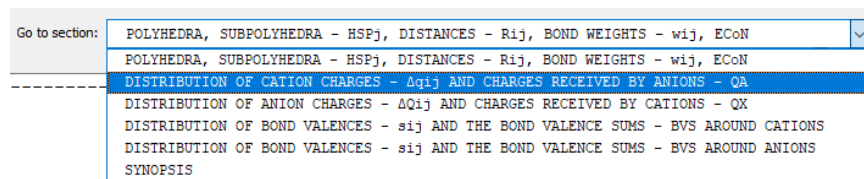
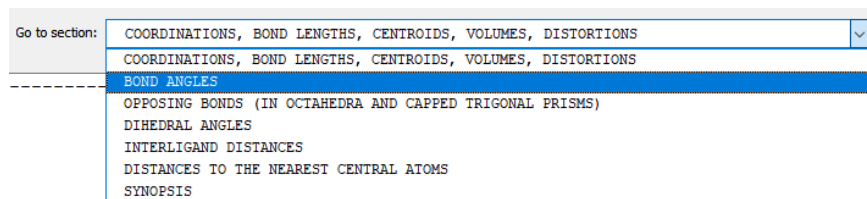


Figure 5. The navigation drop down list for detailed CD-BVS outputs.



The parameters presented in [Section 2.3](#) may be listed at the push of the **Coordination geometry** button. Summary and detailed views are available. The detailed results are organized in six sections and can be scrolled through with a dedicated navigation aid ([Figure 6](#)):



**Figure 6.** The navigation aid for the detailed **Coordination geometry** listing.

The main section of the **Coordination Geometry** output contains the detailed CP data, bond distances, distances to centroid and the symmetry operators responsible for generating the ligands. It also displays the coordinates of the centroid and all the quantities deriving from this concept, including the vector defined by the central atom and the centroid, the radius and volume of the LSF sphere. Various internal and external distortion parameters are also included in this section (example):

COORDINATIONS, BOND LENGTHS, CENTROIDS, VOLUMES, DISTORTIONS						
	X	Y	Z	Distances to: central atom    centroid		Symmetry operator
Pb1	0.0318	0.7500	0.2191			(0,0,0) + (x,y,z)
1. S24	-0.0167	0.7500	0.2601	2.7441	3.1355	(-1,0,0) + (x,y,z)
2. S23	-0.0192	0.2500	0.1806	3.0276	3.1344	(-1,0,0) + (-x,1/2+y,-z)
3. S23	-0.0192	1.2500	0.1806	3.0276	3.1344	(-1,1,0) + (-x,1/2+y,-z)
4. S1	0.0616	0.2500	0.2743	3.0450	3.1360	(0,0,0) + (x,y,z)
5. S1	0.0616	1.2500	0.2743	3.0450	3.1360	(0,1,0) + (x,y,z)
6. S27-Se27	0.0291	0.7500	0.1336	3.3847	3.1374	(0,0,0) + (x,y,z)
7. S30-Se30	0.0965	0.2500	0.2016	3.4258	3.1344	(0,0,0) + (x,y,z)
8. S30-Se30	0.0965	1.2500	0.2016	3.4258	3.1344	(0,1,0) + (x,y,z)
Centroid	0.0393	0.7500	0.2139			
Average distance				3.1407	3.1353	
Standard deviation of distances				0.2459	0.0011	
Central atom - centroid vector				-0.0075	0.0000	0.0052
Central atom - centroid distance				0.3924		
Radius of least-squares fitted circumsphere				3.1353		
Volume of least-squares fitted circumsphere				129.1028		
Linear and volume-based eccentricity				0.1252	0.3304	
Linear and volume-based sphericity				0.9997	0.9990	
Number of polyhedron faces				11		
Faces	Partial volumes					
1 2 3				4.0804		
1 2 4				4.0499		
1 3 5				4.0499		
1 4 5				4.0193		
2 3 6				4.3879		
2 4 7				4.7132		
2 6 7				5.0696		
3 5 8				4.7132		
3 6 8				5.0696		
4 5 7 8				4.2193		
				4.2193		
6 7 8				4.2193		
Volume of polyhedron				54.3428		
Ideal polyhedron approximation				bicapped trigonal prism		
Ideal polyhedron volume				55.9637		
Polyhedron distortion				0.0290		
Baur distortion index				0.0648		
Brown distortion index				0.0590		
Deviation of ECon from CNR				0.0358		

The figures in the **Faces** column represent the indices of the ligands forming the triangular faces of the CP. These indices are found in the coordinates table at the beginning of each record. In the example above, a quadrilateral face is formed by the ligands 4 5 7 8. Details on how ECoN21 establishes the faces of the coordination polyhedron and on how it approximates the ideal polyhedron are given in [Section 4.4](#) of this manual.

A second section of the **Coordination geometry** output, lists all the bond angles formed by each central atom and a pair of ligands in the CP. This section is optional and can be set on or off from the [Calculation Settings](#) dialog. Examples:

#### BOND ANGLES

Pb1	S23	S23	S1	S1	S-Se27	S-Se30	S-Se30
S24	80.96	80.96	76.94	76.94	136.12	138.41	138.41
S23		84.98	91.11	157.90	67.28	85.60	136.87
S23			157.90	91.11	67.28	136.87	85.60
S1				84.38	130.69	64.11	111.41
S1					130.69	111.41	64.11
S-Se27						70.25	70.25
S-Se30							73.30

S1	Bi3	Pb2	Pb1	Pb1
Bi3	92.85	98.14	88.01	159.79
Bi3		98.14	159.79	88.01
Pb2			101.73	101.73
Pb1				84.38

The third section displays the opposing bond distances in octahedral and capped trigonal prisms. The values are used with the discriminating hyperbolae diagrams described by Trömel (1981) and Berlepsch *et al.* (2001). Details on the opposing bond distances meaning and usage are given in [Section 8](#) of this manual. This calculation is optional and only available in the cation-centered description.

#### OPPOSING BONDS (IN OCTAHEDRA AND CAPPED TRIGONAL PRISMS)

Central atom	RX	RY	Angle		Opposing ligands	
As1	2.2316	3.2651	159.96	in plane	S4	S7
	2.3120	3.2609	156.30	in plane	S3	S8
	3.7648	2.2462	168.01	out of plane	S9	S1
Central atom	RX	RY	Angle		Opposing ligands	
As2	2.4073	2.9477	167.52	in plane	S3	S8
	2.2853	3.4295	148.40	in plane	S7	S4
	3.5949	2.2381	166.28	out of plane	S10	S2
	3.7267	2.2381	128.82	out of plane*	S6	S2
Central atom	RX	RY	Angle		Opposing ligands	
Sb1	2.5813	2.8575	171.10	in plane	S8	S9
	2.3795	3.4638	149.54	in plane	S10	S7
	3.5367	2.5056	155.98	out of plane	S7	S5
	3.5278	2.5056	138.60	out of plane*	S9	S5



The next section lists the mean values of the first three shortest bonds and of the next two shortest bonds. These values are used in the discriminatory diagram introduced by Armbruster and Hummel (1987)<sup>1</sup>, described in [Section 9](#) of this manual. The calculation is optional.

#### 123-45 BOND AVERAGES

Central atom	Average123	Average45
Pb1	2.897	3.124
Pb2	3.013	3.126
Pb3	3.022	3.139
Pb4	3.086	3.165
Pb5	3.038	3.152
Pb6	3.003	3.105
Pb7	3.033	3.115
Pb8	2.962	3.173
. . . . .		
As21-Pb21	2.592	2.958
As22-Pb22	2.531	2.807

A fifth section of the **Coordination geometry** listing, enumerates the dihedral angles between each pair of adjacent triangular faces used for calculating the partial volumes of the CP. The tables under this section help in establishing the maximum dihedral angles in the CP and in adjusting the optimal **Maximum dihedral angle** in the [Calculation settings](#) dialog. The departure of these angles from those of the ideal approximant polyhedron might also be worth examining. This calculation is optional.

#### DIHEDRAL ANGLES

Pb	1-S24, 2-S23, 3-S23, 4-S1, 5-S1, 6-S27-Se27, 7-S30-Se30, 8-S30-Se30,		
	1 2 4	1 3 5	2 3 6
1 2 3	120.02	120.02	139.36
	1 2 3	1 4 5	2 4 7
1 2 4	120.02	118.23	136.55
	1 2 3	1 4 5	3 5 8
1 3 5	120.02	118.23	136.55
	1 2 4	1 3 5	4 5 7
1 4 5	118.23	118.23	114.18
. . . . .			
	2 3 6	2 4 7	6 7 8
2 6 7	116.10	137.35	120.43
	1 3 5	3 6 8	5 7 8
3 5 8	136.55	137.35	90.00
	2 3 6	3 5 8	6 7 8
3 6 8	116.10	137.35	120.43
	3 5 8	4 5 7	6 7 8
5 7 8	90.00	180.00	107.45
	1 4 5	2 4 7	5 7 8
4 5 7	114.18	90.00	180.00
	2 6 7	3 6 8	5 7 8
6 7 8	120.43	120.43	107.45

<sup>1</sup> Also in Hummel and Armbruster (1987)

The sixth section contains the ligand-to-ligand distances for each CP (optional):

#### INTERLIGAND DISTANCES

Pb1	S23	S23	S1	S1	S27-Se27	S30-Se30	S30-Se30
S24	3.7533	3.7533	3.6093	3.6093	5.6899	5.7731	5.7731
S23		4.0900	4.3353	5.9601	3.5646	4.3946	6.0034
S23			5.9601	4.3353	3.5646	6.0034	4.3946
S1				4.0900	5.8453	3.4492	5.3503
S1					5.8453	5.3503	3.4492
S27-Se27						3.9186	3.9186
S30-Se30							4.0900

The seventh section lists the distances to the closest neighboring central atoms—within a margin of 5 Å (optional):

#### DISTANCES TO THE NEAREST CENTRAL ATOMS

	X	Y	Z	Distance	Symmetry operator
Pb1	0.0318	0.7500	0.2191		(0,0,0) + (x,y,z)
1. Bi3	0.1050	0.7500	0.3093	4.0798	(0,0,0) + (x,y,z)
2. Pb1	0.0318	-0.2500	0.2191	4.0900	(0,-1,0) + (x,y,z)
3. Pb1	0.0318	1.7500	0.2191	4.0900	(0,1,0) + (x,y,z)
4. Pb28-Bi28	0.1036	0.7500	0.1552	4.1579	(0,0,0) + (x,y,z)
5. Bi24	-0.0617	0.2500	0.2245	4.2146	(-1,0,0) + (-x,1/2+y,-z)
6. Bi24	-0.0617	1.2500	0.2245	4.2146	(-1,1,0) + (-x,1/2+y,-z)
7. Pb23	-0.0550	0.7500	0.1336	4.2521	(-1,0,0) + (-x,1/2+y,-z)
8. Pb2	0.0098	0.2500	0.3147	4.5606	(0,0,0) + (x,y,z)
9. Pb2	0.0098	1.2500	0.3147	4.5606	(0,1,0) + (x,y,z)

The final section is a synoptic table containing the essential coordination and distortion data:

#### SYNOPSIS

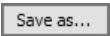
CN	- Coordination number
AV	- Average distance
AVsd	- Standard deviation of distances
Xo,Yo,Zo	- Coordinates of centroid
I,J,K	- Components of vector between central atom and centroid
Δ	- Displacement of central atom from centroid
SRad	- Radius of least-squares fitted circumsphere
SVol	- Volume of least-squares fitted circumsphere
SAVsd	- Standard deviation of distances to centroid
LEcc,VEcc	- Linear and volume-based eccentricity
LSph,VSph	- Linear and volume-based sphericity
PVol	- Volume of coordination polyhedron
IPVol	- Volume of ideal coordination polyhedron
PDist	- Polyhedron volume distortion
ΔR	- Distortion indexes - (Ba)ur, (Br)own
EDEV	- Deviation of ECon from CNR

Cation	CN	AV	AVsd	Xo	Yo	Zo	I	J	K	Δ	SRad	SVol	LEcc	VEcc
Pb1	8	3.141	0.246	0.0393	0.7500	0.2139	-0.0075	0.0000	0.0052	0.392	3.135	129.103	0.001	0.125
Pb2	8	3.174	0.323	-0.0005	0.2500	0.3167	0.0103	0.0000	-0.0020	0.425	3.167	133.037	0.196	0.134
Bi3	6	2.872	0.117	0.1091	0.7500	0.3083	-0.0041	0.0000	0.0010	0.173	2.878	99.844	0.024	0.060
Bi4	6	2.858	0.100	0.0996	0.2500	0.3987	0.0031	0.0000	-0.0017	0.151	2.864	98.445	0.023	0.053
Pb5	7	3.035	0.164	0.2004	0.7500	0.3885	-0.0042	0.0000	0.0044	0.263	3.046	118.426	0.001	0.086
Pb6	8	3.169	0.273	0.1684	0.2500	0.4947	0.0065	0.0000	-0.0064	0.397	3.161	132.301	0.105	0.126
Bi7	6	2.845	0.140	0.2717	0.7500	0.4794	-0.0036	0.0000	0.0036	0.222	2.856	97.615	0.004	0.078
. . . . .														
	LSph	VSph	SAVsd	PVol	IPVol	PDist	ΔR(Ba)	ΔR(Ba)	EDEV	Ideal polyhedron type				
Pb1	0.330	1.000	0.999	54.343	63.382	0.143	0.065	0.059	0.036	bicapped trigonal prism				
Pb2	0.351	0.938	0.814	55.333	65.314	0.153	0.069	0.082	0.058	bicapped trigonal prism				
Bi3	0.170	0.992	0.975	30.968	31.781	0.026	0.033	0.015	0.030	octahedron				
Bi4	0.150	0.992	0.976	30.940	31.336	0.013	0.024	0.012	0.035	octahedron				
Pb5	0.237	1.000	0.999	39.339	37.687	-0.044	0.040	0.024	0.022	monocapped trigonal prism				
Pb6	0.331	0.967	0.900	54.918	64.952	0.154	0.075	0.070	0.114	bicapped trigonal prism				
Bi7	0.215	0.999	0.996	30.436	31.072	0.020	0.027	0.020	0.028	octahedron				
. . . . .														

With the **Autosave results** ☒ checked **on**, whenever the output panel displays a new content, the results are saved in an output file without the user being prompted. Any preexisting file having the same name with the one generated by a specific viewing context will be overwritten without notice. The naming of the output file is designed to preserve the original CIF name to which several suffixes (CC, AC, D, S), suggestive for a specific view mode, are added. Examples:

- *cannizzarite-CC-D.out* – the output file contains the **Detailed** results calculated for the **Cation-Centered** description; the original input file name was *cannizzarite.cif*.
- *argentoliveingite-AC-S.out* – the output file contains the **Summary** listing for the **Anion-Centered** description; the original input file name was *argentoliveingite.cif*.

All output files are saved in the folder wherefrom the input CIF file originated. The output files are in text format. If the file extension (*e.g.*, '.out') and the application which opens it are not recognized, the user should simply double-click on the file name in Windows Explorer and choose Notepad or any other program able to read text files.

By checking the **Autosave results** ☐ **off**, the results can be saved using the  command. In the **Save as** dialog, the user may choose to save the following types of output files:

- ECoN21 detailed CD–BVS results (\*.out) – text format
- ECoN21 summary CD–BVS results (\*.out) – text format
- CSV summary results (\*.csv) – Comma Separated Values format (for import into MSExcel)
- ECoN21 detailed polyhedron geometry (\*.pol) – text format
- ECoN21 summary polyhedron geometry (\*.pol) – text format

The choice for file formats depends on what the results pane is displaying at the moment of saving the file. The **Save as** command allows changing the folders and prevents the accidental overwriting of existing files. In order to preserve the atoms perfectly recognizable in the output, the program keeps the original atom labels found in the CIF file and does not attempt to reorder these atoms, apart from the case when cations and anions are interspersed in the atom list and when atoms sharing the same coordinates, are not listed in succession. The CIF file itself is not modified.

### 3.3 Interpreting the results

The charge distribution calculation performed by ECoN21 is not intended for assessing the overall neutrality of the crystal structure. This information is already embedded in the site population, oxidation number and occupancy fields of the CIF file and it is displayed as the **overall charge balance** and as the **relative charge error** calculated on the basis of the **structure–derived formula**. The program only *distributes* the existing charge and therefore, if it does this distribution correctly, then running a similar calculation based on the computed  $Q_X$  and  $Q_A$  values would yield nothing else but a *reversed* charge balance, *e.g.*:

- Overall charge balance (from structure derived formula): –448.000:447.820
- Overall charge balance (from charge distribution): –447.820:448.000

However, the program does calculate **CD–** and **BVS–derived formulas** to compare with the **structure–derived** one. The estimation of the overall correctness of the crystal structure model and the interpretation of the

oxidation numbers assigned to monoelemental or (heterovalent) mixed sites relies on the following simple criteria:

- the  $Q_X$ ,  $Q_A$ ,  $BVS_X$ , and  $BVS_A$  values should be close to their corresponding formal oxidation numbers  $q_X$  or  $q_A$ , respectively. Consequently, the departure from 1.0 of the  $q_X/Q_X$  and  $q_A/Q_A$  ratios may also be used to assess the matching between the formal and calculated charges. In the cation-centered description, the  $q_X/Q_X$  ratio gives a measure of the overall geometric correctness of the structure (atom coordinates, distances), whereas  $q_A/Q_A$  points to the over- or underbonding effects induced by inadequate calculated charges of the central atoms (*e.g.*, Nespolo *et al.*, 1999, 2001), making it suitable for measuring the effects of compositional changes in the central heterovalent mixed positions. In the anion-centered description, the significance of the two ratios is reversed.
- the mean absolute percentage deviation *MAPD* (Eon and Nespolo 2015) of  $Q_X$ ,  $Q_A$ ,  $BVS_X$  or  $BVS_A$  from the nominal oxidation numbers ( $q_X$  or  $q_A$ ) for the entire structure or selected clusters of atoms. These values should be as close as possible to 0%. It may be roughly estimated that *MAPDs* larger than 10% point out negative issues in the refinement of the crystal structure. Elevated *MAPDs* for global or local ligands should draw attention to potentially misassigned oxidation numbers of the central atoms.

More advanced interpretations may result from the use of collateral parameters calculated by the program, such as  $ECoN_X$  or  $EDEV_X$  and by analyzing their relationship with various geometric parameters of the structure (*e.g.*, the polyhedral distortion).

## 4 Calculation settings

The **Calculation settings...** button opens the following dialog box:

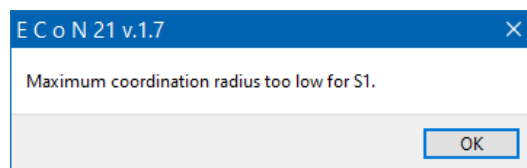
Bond type	Maximum bond length
Ag : S	3.9550
Ag-As : S	3.0170
Ag-Pb : S	3.4116
As : S	3.9914
As-Pb : S	3.9268
Pb : S	3.9422

The dialog allows the adjustment of parameters related to the coordination radii, iteration procedures, approximation of the ideal coordination polyhedra and opposing bonds calculation. Controls are also available for choosing whether some of the Coordination Geometry calculations will be carried out or not. The background and use of these categories are explained in the following sections. Opposing bonds settings are explained in [Section 8](#).

### 4.1 The coordination radii

ECoN21 builds the coordination polyhedra around a central atom, using **global**, **bond-type specific** or **polyhedron specific** coordination radii. By choosing the **Global coordination thresholds** option, the user can set a general **Maximum coordination radius** which will establish a limit for searching distances around *all* the central atoms in the structure, as well as a **Hydrogen coordination radius**.

The maximum preset of the global coordination radius is conventionally set to 5 Å, although it makes little sense to raise this threshold so high. The lower limit of the global coordination radius requires that a minimum  $CN = 1$  is available. If the program does not find at least one ligand around a central atom, it will generate an error message:



With the **Bond-type specific thresholds** option selected, the user can modify the coordination radii for each type of chemical bond, separately. Once the table of chemical types of bonds is activated for the first time, it will suggest the most probable thresholds. Each bond type can be selected and edited.

Manual setting of coordination is also possible by checking the **Polyhedron specific thresholds** radio button and by adjusting the maximum bond length for each polyhedron:

Central atom: As1      Coordination number: 5

Ligand No.	Atoms in the coordination sphere	Distances
1	S4	2.2215
2	S1	2.2492
3	S3	2.3192
4	S8	3.1991
5	S7	3.2448
	Sb3	3.6465
	Pb6-As6	3.7844
	As2	3.8691
6	S9	3.8691

Buttons: >> Anion centered, < Previous, Next >, Reset, OK, Cancel

Tooltip: Double click to set the maximum bond length

The dialog allows the setting of the coordination number by double clicking on what is to be considered the maximum bond length for a given polyhedron and which can be different from other maxima in other polyhedra. The dialog displays the list of atoms—both ligands and central atoms—lying inside the coordination sphere determined by the current global **Maximum coordination radius**. The ligands are numbered and the current *CN* is displayed. Central atoms may be seen sequentially by pressing the **Next >** or the **< Previous** button. The **Central atom** drop down list allows rapid navigation throughout the coordination polyhedra. The **Reset** button restores the coordinations to the state found at the opening of the dialog. The manual setting of coordination overrides all the other coordination thresholds.

Note that the actual limitation of the coordination number is made by setting a *distance limit*. If the bond selected as a threshold is followed by a bond of similar length (8 in the example below), that bond will also be included in the CP:

Central atom: Pb2      Coordination number: 7

Ligand No.	Atoms in the coordination sphere	Distances
1	S9	2.9187
2	S9	2.9187
3	S21	3.0555
4	S6	3.1463
5	S24	3.1791
6	S24	3.1791
7	S3	3.2967
8	S3	3.2967

Buttons: >> Anion centered, < Previous, Next >, Reset, OK, Cancel

Red arrow points to the 8th ligand (S3) with distance 3.2967.

The dialog gives also the option of limiting the coordination radius to the distance measured to the nearest central atom in a neighboring CP (when such central atoms occur inside the coordination sphere defined by the global or bond-type specific radius), as well as of eliminating ligands with zero-weight bonds from the coordination polyhedra:

☒ Limit coordination radius using distance to the nearest central atom

With this control **on**, the calculation ignores ligands located farther than the nearest neighboring central atom. The user can check if central atoms are included in the 1<sup>st</sup> coordination sphere by visiting [the 7<sup>th</sup> section](#) of the **Coordination geometry** listing.

☒ Exclude ligands with zero-weight bonds from coordination polyhedra

With this control checked, the program builds the coordination polyhedra using ligands with non-zero bond weights. A preliminary calculation is performed using the default **Maximum coordination radius** followed by the adjustment of the *CN* for each polyhedra, using the non-zero-weight occurrences.

By setting the coordination radius too low, no detectable ligands might be left around a central atom. If set too high, then too many ligands will be counted in the coordination polyhedra and the quality of results will be affected. Several cases are given further on. AMCSD 0002226—and reference therein:

```
_chemical_formula_sum 'Fe H O2'
_cell_length_a 9.9134
_cell_length_b 3.0128
_cell_length_c 4.5800
_cell_angle_alpha 90
_cell_angle_beta 90
_cell_angle_gamma 90
_symmetry_space_group_name_H-M 'P n m a'
```

```
loop_
_space_group_symop_operation_xyz
  'x,y,z'
  'x,1/2-y,z'
  '-x,1/2+y,-z'
  '1/2-x,1/2+y,1/2+z'
  '1/2+x,1/2-y,1/2-z'
  '1/2+x,y,1/2-z'
  '1/2-x,-y,1/2+z'
  '-x,-y,-z'
```

```
loop_
_atom_site_label
_atom_site_type_symbol
_atom_site_fract_x
_atom_site_fract_y
_atom_site_fract_z
_atom_site_occupancy
Fe Fe3+ 0.14590 0.25000 -0.04860 1
H H1+ -0.10100 0.25000 -0.39900 1
O1 O2- -0.19900 0.25000 0.28500 1
O2 O2- -0.05170 0.25000 -0.19600 1
```

In this case, running the structure at a global **Maximum coordination radius** of 4 or 3 Å makes little difference in the charge distribution results because the bonds longer than 3 Å, filter themselves out due to their zero-weight:

Central atom	Site population	CN	qX	Ligand	qA	Rij	wij	
Fe	1.000.Fe	17	3.000	O1	-2.000	1.9284	1.2015	
				O1	-2.000	1.9284	1.2015	
				O1	-2.000	1.9549	1.1205	
				O2	-2.000	2.0720	0.7740	
				O2	-2.000	2.0967	0.7053	
				O2	-2.000	2.0967	0.7053	
				O2	-2.000	3.2179	0.0000	
				O1	-2.000	3.5915	0.0000	
				O1	-2.000	3.5915	0.0000	
				O2	-2.000	3.6565	0.0000	
				O2	-2.000	3.6565	0.0000	
				O1	-2.000	3.7067	0.0000	
				O1	-2.000	3.7450	0.0000	
				O1	-2.000	3.8441	0.0000	
				O1	-2.000	3.8441	0.0000	
				O2	-2.000	3.8873	0.0000	
				O2	-2.000	3.8873	0.0000	
					wRav:	1.9947	ECoNX:	5.7080
							EDEV:	0.6642

However, the bond valence sum will get a contribution even from these distant ligands and will generate a slight but undesirable overbonding effect:

Central atom	Site population	qX	Ligand	Rij	sij	ERij
Fe	1.000.Fe	3.000	O1	1.9284	0.6327	1.9470
			O1	1.9284	0.6327	1.9470
			O1	1.9549	0.5889	1.9735
			O2	2.0720	0.4292	2.0906
			O2	2.0967	0.4014	2.1154
			O2	2.0967	0.4014	2.1154
			O2	3.2179	0.0194	3.2366
			O1	3.5915	0.0071	3.6101
			O1	3.5915	0.0071	3.6101
			O2	3.6565	0.0059	3.6751
			O2	3.6565	0.0059	3.6751
			O1	3.7067	0.0052	3.7253
			O1	3.7450	0.0047	3.7636
			O1	3.8441	0.0036	3.8628
			O1	3.8441	0.0036	3.8628
			O2	3.8873	0.0032	3.9059
			O2	3.8873	0.0032	3.9059
Distortion index (Brown): 0.7182				BVS(Fe): 3.1550		

If the **Maximum coordination radius** is justifiably set to 3 Å, then the bond valence sum will get closer to the formal oxidation number, *i.e.*, +3:

Central atom	Site population	qX	Ligand	Rij	sij	ERij
Fe	1.000.Fe	3.000	O1	1.9284	0.6327	1.9389
			O1	1.9284	0.6327	1.9389
			O1	1.9549	0.5889	1.9654
			O2	2.0720	0.4292	2.0824
			O2	2.0967	0.4014	2.1072
			O2	2.0967	0.4014	2.1072
Distortion index (Brown): 0.0079				BVS (Fe): 3.0863		



Sometimes, the difference between choosing the default 4 Å global radius and a lower value is more significant. In the following example of muscovite (AMCSD 0000854—and reference therein), for a 4 Å coordination radius, the *CN* around potassium is 12 and the long bonds are still strong enough to make the more distant ligands receive a fraction of the central charge:

Central atom	Site population	CN	qX	Ligand	qA	Rij	wij
K	1.000.K	12	1.000	O3	-2.000	2.8501	1.2516
				O3	-2.000	2.8501	1.2516
				O4	-2.000	2.8654	1.2203
				O4	-2.000	2.8654	1.2203
				O5	-2.000	2.8976	1.1545
				O5	-2.000	2.8976	1.1545
				O4	-2.000	3.2854	0.4406
				O4	-2.000	3.2854	0.4406
				O3	-2.000	3.2939	0.4282
				O3	-2.000	3.2939	0.4282
				O5	-2.000	3.5040	0.1867
				O5	-2.000	3.5040	0.1867
wRav: 2.9734						ECoNX: 9.3639	
						EDEV: 0.2197	

Also, the Si1–Al1 position—normally with a tetrahedral coordination—appears with a *CN* = 13 and anomalously bonded to OH<sup>−</sup> groups:

Central atom	Site population	CN	qX	Ligand	qA	Rij	wij		
Sil-Al1	0.750.Si:0.250.Al	13	3.750	O1	-2.000	1.6338	1.0421		
				O5	-2.000	1.6439	1.0052		
				O3	-2.000	1.6515	0.9775		
				O4	-2.000	1.6529	0.9724		
				O2	-2.000	3.2893	0.0000		
				O2	-2.000	3.3225	0.0000		
				O2	-2.000	3.6638	0.0000		
				O5	-2.000	3.7525	0.0000		
				O4	-2.000	3.8529	0.0000		
				O3	-2.000	3.8880	0.0000		
				-----					
				HSP1:		wRav1: 1.6453		ECoN1: 3.9972	
				OH6		-1.000		3.2278	
				OH6		-1.000		3.4265	
				OH6		-1.000		3.7272	
				-----					
				HSP2:		wRav2: 3.3822		ECoN2: 2.6525	
				-----					
						EDEV: 0.4885			

Other positions are overcoordinated, too, and the overall *MAPD* for cations is quite high: 6.17%. However, by setting the **Maximum coordination radius** to 3 Å, the *CN*s become normal and the *MAPD* gets significantly lower: 1.03%:

Central atom	Site population	CN	qX	Ligand	qA	Rij	wij
K	1.000.K	6	1.000	O3	-2.000	2.8501	1.0422
				O3	-2.000	2.8501	1.0422
				O4	-2.000	2.8654	1.0101
				O4	-2.000	2.8654	1.0101
				O5	-2.000	2.8976	0.9431
				O5	-2.000	2.8976	0.9431
							EDEV: 0.0016

Central atom	Site population	CN	qX	Ligand	qA	Rij	wij
Si1-Al1	0.750.Si:0.250.Al	4	3.750	O1	-2.000	1.6338	1.0421
				O5	-2.000	1.6439	1.0052
				O3	-2.000	1.6515	0.9775
				O4	-2.000	1.6529	0.9724

wRav: 1.6453 ECoNX: 3.9972  
EDEV: 0.0007

Cation	CN	ECoN	EDEV	qX	QX	qX/QX	BVS
K	6	5.991	0.002	1.000	0.987	1.013	0.690
Si1-Al1	4	3.997	0.001	3.750	3.723	1.007	3.831
Si2-Al2	4	3.999	0.000	3.750	3.734	1.004	3.900
Al3	6	5.996	0.001	3.000	3.050	0.984	-

MAPD: 1.03% n/a

Anion	qA	QA	qA/QA	BVS
O1	-2.000	-1.979	1.011	1.885
O2	-2.000	-1.952	1.025	1.882
O3	-2.000	-2.006	0.997	2.021
O4	-2.000	-2.015	0.992	2.028
O5	-2.000	-2.062	0.970	2.062
O-H6	-1.000	-0.986	1.014	-

MAPD: 1.50% n/a

Sometimes, setting a single, global **Maximum coordination radius**, no matter how much adjusted, fails to generate correct coordination polyhedra. Example:  $\text{La}_2\text{SeSiO}_4$  (Brennan and Ibers, 1991)—COD2000322 (fragment):

```

_cell_length_a      6.279(4)
_cell_length_b      7.306(5)
_cell_length_c     11.177(7)
_cell_angle_alpha    90
_cell_angle_beta     90
_cell_angle_gamma    90

loop_
_symmetry_equiv_pos_as_xyz
'x,y,z'
'-x,1/2+y,z'
'x,1/2-y,1/2+z'
'x,y,1/2-z'
'-x,-y,-z'
'x,1/2-y,-z'
'-x,1/2+y,1/2-z'
'-x,-y,1/2+z'

loop_
_atom_site_label
_atom_site_type_symbol
_atom_site_fract_x
_atom_site_fract_y
_atom_site_fract_z
_atom_site_occupancy
La1 La3+  0.12424(5)  0.03774(4)  0.2500  0.29 1
La2 La3+  0.60658(5)  0.2500  0.0000  0.379 1
Se Se2-  0.41697(10)  0.40157(9)  0.2500  0.469 1
Si Si4+  0.1102(3)  0.2500  0.0000  0.32 1
O1 O2-  0.0479(5)  0.7686(4)  0.1161(3)  0.39 1
O2 O2-  0.2654(5)  0.0783(4)  0.0328(3)  0.39 1

```

A **Maximum coordination radius** of 4 Å determines Si to form a heteroligand coordination polyhedron with four oxygen atoms and two—very distant—Se atoms.

Central atom	Site population	CN	qX	Ligand	qA	R <sub>ij</sub>	w <sub>ij</sub>				
Si	1.000.Si	10	4.000	O2	-2.000	1.6302	1.0167				
				O2	-2.000	1.6302	1.0167				
				O1	-2.000	1.6395	0.9828				
				O1	-2.000	1.6395	0.9828				
				O2	-2.000	3.3837	0.0000				
				O2	-2.000	3.3837	0.0000				
				O1	-2.000	3.7692	0.0000				
				O1	-2.000	3.7692	0.0000				
				HSP1:				wRav1:	1.6348	ECoN1:	3.9989
				Se	-2.000	3.5701	1.0000				
Se	-2.000	3.5701	1.0000								
HSP2:				wRav2:	3.5701	ECoN2:	2.0000				
						ECoNX:	5.9989				
						EDEV:	0.4001				

Reducing the global **Maximum coordination radius** to 3 Å, that is, lower than the Si–O distance generating the first zero-weight bond, is not an option because all the bonds formed by Se with La measure over this value:

Central atom	Site population	CN	qA	Ligand	qX	Rij	wij
Se	1.000.Se	7	-2.000	La1	3.000	3.0476	1.3995
				La1	3.000	3.2324	1.0563
				La2	3.000	3.2329	1.0554
				La2	3.000	3.2329	1.0554
				La1	3.000	3.5407	0.5312
				La2	3.000	3.7827	0.2399
				La2	3.000	3.7827	0.2399
				-----			
wRav: 3.2629						ECoNX: 5.5776	
						EDEV: 0.2032	

Not being able to determine the coordination of Se in the anion-centered description, the program will generate a specific error message. The solution is to choose the **Bond-type specific thresholds** option in the [Calculation settings](#) dialog and modify the Si : Se threshold to a value above 3 Å. The Si : O maximum bond length may be modified too, by setting it under 3 Å. In this way, the oxygen atoms with zero bond weights will be filtered out and a correct coordination number for Si (4 instead of 8) will be obtained.

The coordination number is especially important in the calculation of  $EDEV_X$  and of the parameters describing the coordination geometry. Therefore it must be carefully observed when choosing bond length thresholds.

## 4.2 Iteration of weighted average distance

By default, ECoN21 uses an iterated value of the weighted average bond length  $\bar{R}_j$ , but the calculation of non-iterated weighted average bond length and all related variables ( $w_{ij}$ ,  $ECoN_X$ ) is also possible. Thus, the computation follows the original method applied by Hoppe *et al.* (1989) and later by Nespolo *et al.* (1999), and allows direct comparisons with the values calculated by the program VESTA 3. For slightly distorted polyhedra the results obtained from the two approaches should not be significantly different.

The recommended setting is to leave the ☒ **Use iterated weighted average distance** control checked.

### 4.3 CD iteration methods and convergence criteria

Crystal structures that are heteroligand in both cation- and anion-centered descriptions undergo an iteration process meant to balance the distribution of charges to chemically different ligands. The iteration may be carried out either with the native ECoN21 method which uses the  $\Delta Q_j/\Delta q_j$  ratio to correct the starting  $\Delta q_{Xij \rightarrow A}$  values for a new iteration cycle (Equations 10–12), or with the swap method derived by Nespolo (2016) and included in the CHARDI2015 program. The choice for the latter option is made simply by checking on the ☒ Use CHARDI2015 iteration method control.

The results from the two methods should not be significantly different. However, the number of iteration cycles in either case may be dissimilar and influenced by the chosen convergence criteria. The classic way to end the iteration (Nespolo, 2016) relies on the difference  $D$  between  $\Delta Q(ij \rightarrow r)$  calculated in both cation- and anion-centered descriptions, which, in terms of ECoN21 notation, reduces to  $D = \Delta q_j - \sum \Delta Q_{ij \leftarrow x}$ . Instead, the ECoN21 method uses the difference  $D = {}^N\Delta Q_j - {}^{N-1}\Delta Q_j$ , calculated for the central atoms, without resorting concomitantly to a 'ligand-centered' environment. The default threshold for this difference is 0.005, but this can be modified with the Calculation settings dialog.

The number of iteration cycles increases for lower thresholds and with the number of CPs in the crystal structure. However, the behavior of the two iteration methods is different. The CHARDI2015 method tends to generate fewer iteration cycles and with a lower but discontinuous variation of intermediate *MAPDs*, whereas ECoN21 produces more cycles and a continuous decrease of *MAPDs* (Figure 7).

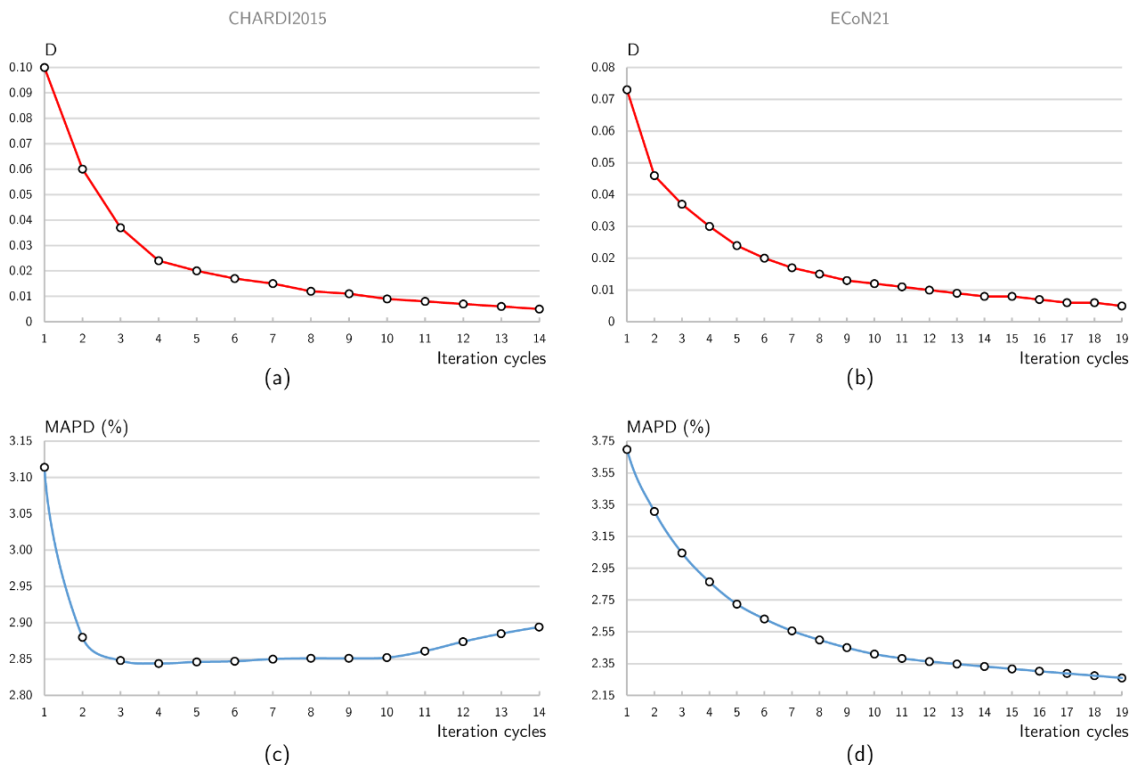


**Figure 7.** Evolution of difference  $D$  during the CD iteration of 7H-12Q cannizzarite (Topa et. al., 2010) for CHARDI2015 (a) and ECoN21 (b) methods. The modification of *MAPD* during the iteration process for CHARDI2015 and ECoN21 is shown in (c) and (d).

Following the ECoN21 method, crystal structures with larger number of polyhedra will tend to yield better *MAPD* results than smaller structures, because they must go through a lot more iterations and thus, the deviating charges will have more chances to level off. Some polyhedra will always be left behind, thus forcing new cycles of iteration and eventually making the calculation prone to artificial results. Too many iterations will also yield 'better' *MAPDs* but will hide potential problematic features of the structure. Therefore, it is not recommended to use the ECoN21 iteration with  $\Delta D_j$  difference thresholds that are lower than the default value of 0.005, especially if the structure contains many CPs.

A more conservative option is to end the iteration when the *MAPD* for a new cycle, stops improving with more than a certain percentage (*e.g.*, 1%) in comparison to the previous cycle. In general, the *MAPD* improves significantly in the first two or three iteration cycles, after which it decreases much more slowly. Using this option ensures that the iteration stops shortly after the CD anomalies produced by the default over-weighting of bonds to single, 'exotic' ligands are neutralized. By stopping the iteration this early, deviating charges will have less chances to adjust and thus, to obliterate potential flaws of the structure.

A final, radical way to stop the iteration—augmenting the effects described for the second option—is to allow only a single iteration cycle.

## 4.4 Approximation of the ideal polyhedron

During the **Coordination geometry** calculations, ECoN21 attempts to establish the ideal polyhedra of maximum volume which are inscribable in the LSF spheres of each CP in the structure, using the *CN* and the number of CP faces. The volume of the ideal polyhedron is used to calculate the volume distortion (Equation 27). Even though the program finds the right ideal polyhedra in most cases, the user should check the suggested shape against a crystal structure visualization program. Better results are obtained if the coordination radius thresholds are set in such a way that only tightly bonded ligands are included in the CP (*e.g.*, having non-zero bond weights). If the program has determined the ideal polyhedron type wrongly, then, after visually deciding upon the right shape, the user should either impose a lower CN or use the values in Table 1 to calculate the ideal volume.

For each type of polyhedra listed in the table, the ratios between the volumes of the LSF 'circumsphere' and of the ideal polyhedron are different and so will be the values of the real polyhedron volume distortion. For instance, the coordination polyhedron around As15 in the crystal structure of baumhauerite (Engel and Nowacki, 1969), at a global coordination radius of 4 Å, can be approximated by two ideal shapes: a 'split octahedron' with S25–S27–S28 and S29–S31–S32 forming the bases of the trigonal prism and with the S33 atom as the apex of the capping pyramid (Figure 8a), or a pentagonal bipyramid with S27 and S32 as the polar vertices (Figure 8b). The former approximation is achieved by merging pairs of triangular faces located on the uncapped sides of the trigonal prism and forming large dihedral angles: 162.8 and 168.0°. The 'split octahedron' approximation will generate an absolute volume distortion of 0.001 whereas the pentagonal bipyramid will yield a volume distortion of 0.130. However, there might be cases when the pentagonal pyramid is a better approximation. The user can switch between the two options by adjusting the Minimum dihedral angle in the Calculation settings dialog. For the example above, setting a value of 160° will trigger the merging of the triangular faces on the uncapped sides of triangular prism and the reduction of polyhedral faces from 10 to 8 (*i.e.*, 'split octahedron' in this case). On the contrary, a value of 179–180° will hinder the convolution of these faces so that the ideal polyhedron will be approximated by a pentagonal bipyramid.

**Table 1.** Maximal volumes of ideal polyhedra as a function of the LSF 'circumsphere' volumes (Makovicky E., Balić-Žunić T. 1998). Shaded rows indicate the polyhedral volumes that are used by default in the calculation of volume distortion for a certain *CN*, when the program cannot establish the ideal polyhedron.

<i>CN</i>	Number of faces	Ideal polyhedron type	Ideal polyhedron volume <sup>†</sup>
3	1 (+3)	trigonal pyramid*	$V_s/8.1621$
4	4	tetrahedron	$V_s/8.1621$
4	1 or 2 (+4)	square pyramid*	$V_s/5.3014$
5	4	tetrahedron**	$V_s/8.1621$
5	5	square pyramid	$V_s/5.3014$
5	6	trigonal bipyramid	$V_s/4.8368$
6	5	trigonal prism	$V_s/4.1888$
6	8	octahedron	$V_s/3.1416$
7	8	monocapped trigonal prism	$V_s/3.1424$
7	8	'split octahedron'	$V_s/3.0491$
7	10	pentagonal bipyramid	$V_s/2.6427$
8	6	cube	$V_s/2.7206$
8	10	square antiprism	$V_s/2.3069$
8	11	bicapped trigonal prism	$V_s/2.4891$
8	12	hexagonal bipyramid	$V_s/4.8368$
9	14	tricapped trigonal prism	$V_s/2.0496$
12	8 or 14	hexagonal (anti)prism	$V_s/2.0944$
12	14	cubeoctahedron	$V_s/1.7772$
12	20	icosahedron	$V_s/1.6516$

<sup>†</sup>  $V_s$  – volume of the LSF 'circumsphere'

\* Central atom is out of the plane of ligands and occupies the apex of a trigonal or square pyramid. The numbers outside the parantheses count the faces formed on ligand vertices, whereas those inside the parantheses count the faces formed by the apical 'central atom' and the ligands. The faces formed on ligand vertices are the only ones used for calculating the polyhedral volumes.

\*\* One or more vertices are approximated from binary split positions. It may apply to other *CNs*, too.

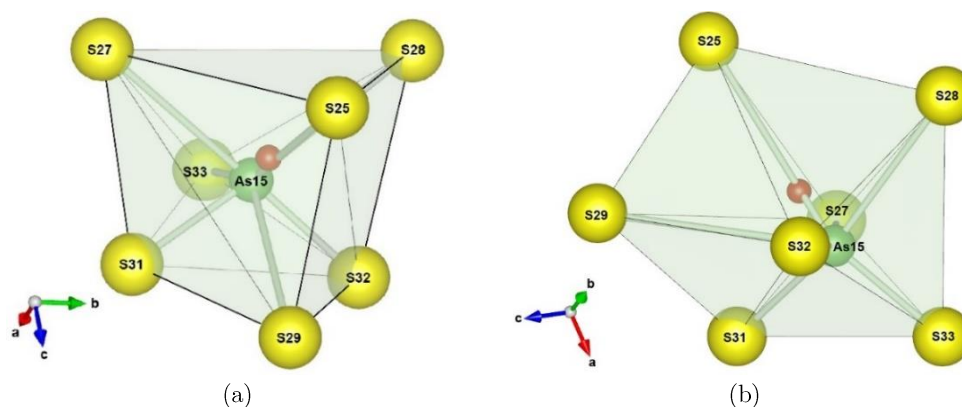


**Figure 8.** The coordination polyhedron of As15 in the crystal structure of baumhauerite (Engel and Nowacki, 1969) seen as a 'split octahedron' with pairs of triangular faces merged into single quadrilateral ones (thicker outlines) (a) or as a pentagonal bipyramid (b). The red sphere denotes the centroid.

Note however, that setting the **Minimum dihedral angle** limit too low (*e.g.*,  $150^\circ$  for the case under scrutiny), will force the merging of other faces (*e.g.*, S29–S31–S33–S32) beside the ones belonging to the uncapped trigonal prism sides and the program will fail to identify the correct ideal polyhedron.

Examination of the **Dihedral angles** in [Section III](#) of the **Coordination geometry** listing may offer a hint on this minimum value.

The choice between the monocapped trigonal prism and the 'split octahedron' is made automatically by comparing the displacements of the central atom from the centroid and from the best plane through the ligands forming the base of the capping pyramid. If the distance from the centroid to the central atom is smaller than the distance to the best plane, then the CP will be a monocapped trigonal prism (Figure 9a). The opposite situation will define a 'split octahedron' (Figure 9b)

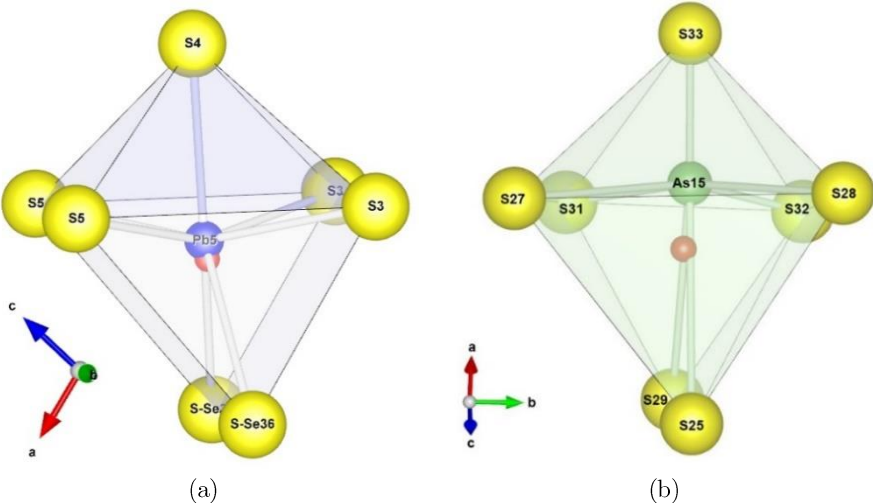


**Figure 9.** The monocapped trigonal prism around Pb5 in 7H-12Q cannizzarite (Topa *et al.* 2010) (a) and the 'split octahedron' around As15 in the crystal structure of baumhauerite (Engel and Nowacki, 1969) (b). The difference is decided by the displacements of the central atom from the centroid (red sphere) and from the best plane through the ligands describing the base of the pyramid cap.

If the global **Maximum coordination radius** is set to 3.5 Å, then the *CN* of As15 changes from 7 to 5 and a similar ambiguity occurs now between a square pyramid (Figure 10a) and a trigonal bipyramid (Figure 10b) as the ideal polyhedron. In the first case, the two triangular faces of the base yield a 175.2° dihedral angle and—with an appropriate **Minimum dihedral angle** setting—can be merged to form the quadrilateral base of the ideal pyramid. The volume distortion for the square pyramid is 0.2661 while for the trigonal bipyramid is slightly larger: 0.3304.

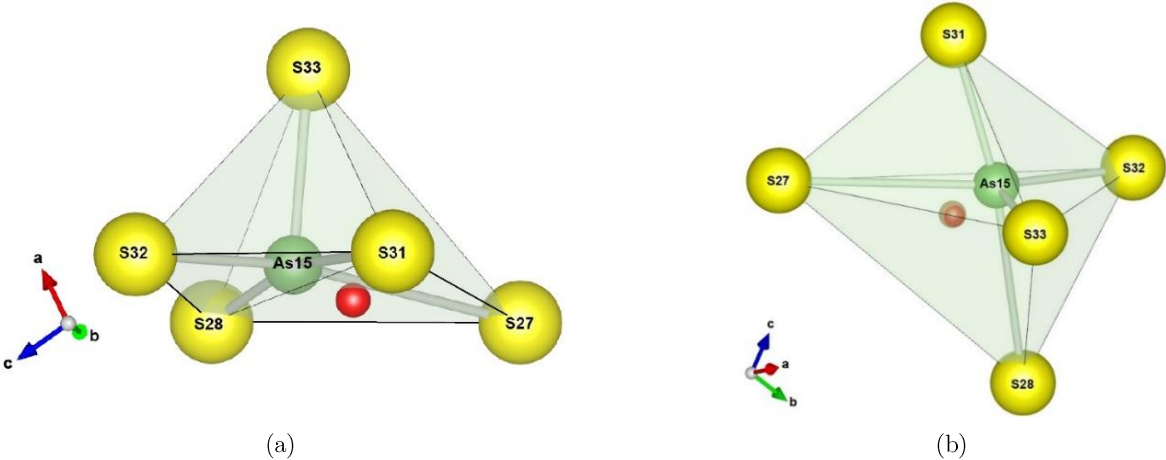


**Figure 10.** Alternative descriptions of the ideal polyhedron type around As15 in the crystal structure of baumhauerite (Engel and Nowacki, 1969) for *CN* = 5: (a) square pyramid obtained by merging of S28-S31-S32 and S27-S28-S31 faces into a quadrilateral face (thicker outline); (b) trigonal bipyramid. The red sphere represents the centroid.



In some rare cases, a unique **Minimum dihedral angle** setting will not suffice to flatten all the pairs of faces with large dihedral angles and the program will not be able to get the ideal shape of certain polyhedra. In such cases, the ideal shapes will be listed with a 'not applicable' tag and the program will choose a default ideal polyhedron yielding the maximum volume for the current *CN*.

In order to identify the ideal CP shape, polyhedra with binary split ligand positions—most likely to be found in anion-centered descriptions—are approximated by merging the pair of ligands into a single, average position. The merging of ligands does not affect other quantities describing the coordination geometry (*CN*, coordinates of the centroid, polyhedral volume, *etc.*). The **Maximum distance between atoms in split positions** setting in the **Calculation settings** dialog helps in adjusting the distance limits for applying such approximations. Values between 0.2 and 1.5 Å are accepted. Example: in the anion-centered description, the S9 position in rathite ('rath 1', Topa and Kolitsch, 2018) is surrounded by three metal split positions: 2 x As5–Ag (distance 0.638 Å) and Sb3–As3 (distance 0.351 Å) (**Figure 11a**). Under a default **Maximum distance between atoms in split positions** of 0.8 Å, the three split positions are merged (**Figure 11b**), thus allowing the program to find the closest ideal shape of the CP (square pyramid in this case). If these positions are kept unmerged (*e.g.*, **Maximum distance...set to 0.2 Å**), the program will fail to identify any plausible ideal shape, volume and distortion.

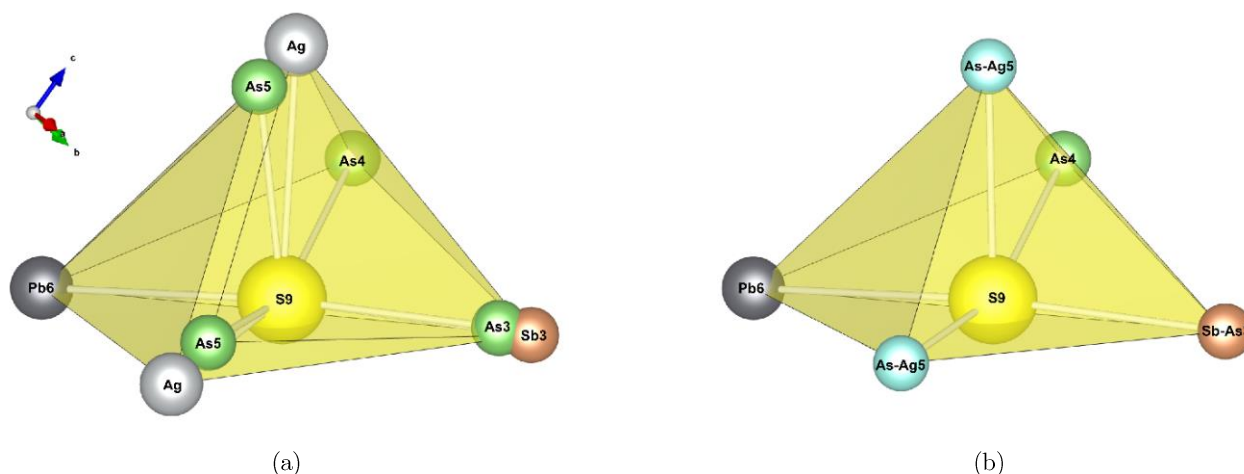


**Figure 11.** The coordination polyhedron of S9 in the crystal structure of rathite ('rath 1', Topa and Kolitsch, 2018) with three split ligand positions (a). These positions are merged (b) for a better approximation of the ideal polyhedron (square pyramid). The ideal shape was obtained with a **Minimum dihedral angle...** of 160° which allowed the two basal faces (As5,Ag5–Pb6–Sb3,As3 and As4–Pb6–Sb3,As3) to be merged into a single one. Any value over this angle would have led to a trigonal bipyramid and to a slightly higher external distortion value.



## 5 Input file requirements

The only type of input accepted by ECoN21 is a CIF file which should contain all the data necessary for the CD and BVS analysis. ECoN21 is fairly flexible when reading a CIF file and in most cases, no intervention from the user is necessary. However, if an error occurs, the user is made aware of its source. Several CIF formats have been tested so far, including ICSD, AMCSD, COD, Jana2006 (Petříček *et al.* 2006) etc. Depending on the source, it may be sometimes necessary to add the oxidation numbers, occupancies *etc.* by hand (see [Section 5.9](#) on how to handle an incomplete CIF file). The following sections describe the information which should be included in the input CIF file (with examples).

### 5.1 Unit cell parameters

```
_cell_length_a 8.5197(4)
_cell_length_b 42.461(2)
_cell_length_c 16.293(8)
_cell_angle_alpha 83.351(2)
_cell_angle_beta 90.958(2)
_cell_angle_gamma 84.275(2)
```

The space group is optional, but it may prove useful if symmetry operators are missing altogether and need to be identified later.

### 5.2 Symmetry operators

Symmetry operators can appear in either of these syntaxes:

a) (flags and cardinal column)

loop_ _space_group_symop_id _symmetry_equiv_pos_as_xyz	loop_ _symmetry_equiv_pos_site_id _symmetry_equiv_pos_as_xyz
1 'x, y, z'	1 'x, y, z'
2 '-x, -y, -z'	2 '-x, -y, -z'
3 '-x+1/2, -y, z+1/2'	3 '-x+1/2, -y, z+1/2'
4 'x+1/2, y, -z+1/2'	4 'x+1/2, y, -z+1/2'
5 'x+1/2, -y+1/2, -z+1/2'	5 'x+1/2, -y+1/2, -z+1/2'
6 '-x+1/2, y+1/2, z+1/2'	6 '-x+1/2, y+1/2, z+1/2'
7 '-x, y+1/2, -z'	7 '-x, y+1/2, -z'
8 'x, -y+1/2, z'	8 'x, -y+1/2, z'

b) (flags)

loop_ _space_group_symop_operation_xyz	loop_ _symmetry_equiv_pos_as_xyz
'x, y, z'	'x, y, z'
'-x, -y, -z'	'-x, -y, -z'
'-x+1/2, -y, z+1/2'	'-x+1/2, -y, z+1/2'
'x+1/2, y, -z+1/2'	'x+1/2, y, -z+1/2'
'x+1/2, -y+1/2, -z+1/2'	'x+1/2, -y+1/2, -z+1/2'
'-x+1/2, y+1/2, z+1/2'	'-x+1/2, y+1/2, z+1/2'
'-x, y+1/2, -z'	'-x, y+1/2, -z'
'x, -y+1/2, z'	'x, -y+1/2, z'

c) (no quotes and no blank spaces)

```
loop_
_symmetry_equiv_pos_as_xyz
x,y,z
-x,-y,-z
-x+1/2,-y,z+1/2
x+1/2,y,-z+1/2
x+1/2,-y+1/2,-z+1/2
-x+1/2,y+1/2,z+1/2
-x,y+1/2,-z
x,-y+1/2,z
```

The individual symmetry operators should be separated by commas. Quotes and blank spaces are not mandatory. The order of operators does not matter.

### 5.3 Atom labels

These are read from a dedicated column in the coordinates table and can be any succession of characters, but should not contain the asterisk sign (\*) as the leading character, as this is reserved for tagging symmetry generated atoms. As a general rule, there should be no blank line between the flags and the actual coordinates table. Examples:

```

_atom_site_label
_atom_site_type_symbol
_atom_site_Wyckoff_symbol
_atom_site_fract_x
_atom_site_fract_y
_atom_site_fract_z
_atom_site_B_iso_or_equiv
_atom_site_occupancy
Tl1 Tl1+ a 0.6573(2) 0.02978(4) 0.82387(12) 0.0321(4) 1
. . . . .
Sb1 Sb3+ a 0.6967(4) -0.01061(6) 0.58114(17) 0.0365(7) 0.8
Pb1 Pb2+ a 0.6967(4) -0.01061(6) 0.58114(17) 0.0365(7) 0.2
Pb2 Pb2+ a 0.1897(4) -0.01719(6) 0.58657(17) 0.0403(9) 0.861(15)
. . . . .
S1 S2- a -0.0910(15) 0.9865(2) 0.9560(6) 0.031(2) 1
S2 S2- a 0.4002(11) 0.9911(2) 0.9681(6) 0.0187(17) 1

_atom_site_label
_atom_site_type_symbol
_atom_site_Wyckoff_symbol
_atom_site_fract_x
_atom_site_fract_y
_atom_site_fract_z
_atom_site_B_iso_or_equiv
_atom_site_occupancy
Me1 Tl1+ a 0.6573(2) 0.02978(4) 0.82387(12) 0.0321(4) 1
. . . . .
Me2a Sb3+ a 0.6967(4) -0.01061(6) 0.58114(17) 0.0365(7) 0.8
Me2b Pb2+ a 0.6967(4) -0.01061(6) 0.58114(17) 0.0365(7) 0.2
Me3 Pb2+ a 0.1897(4) -0.01719(6) 0.58657(17) 0.0403(9) 0.861(15)
. . . . .
A1 S2- a -0.0910(15) 0.9865(2) 0.9560(6) 0.031(2) 1
A2 Se2- a 0.4002(11) 0.9911(2) 0.9681(6) 0.0187(17) 1

```

### 5.4 Atom symbols

Valid chemical symbols followed or not by the oxidation number: Pb2+, Sb3+, S2-, Se2-, *etc.* or Pb, Sb, S, Se *etc* should appear in the CIF file. Example:

```

_atom_site_label
_atom_site_type_symbol
_atom_site_Wyckoff_symbol
_atom_site_fract_x
_atom_site_fract_y
_atom_site_fract_z
_atom_site_B_iso_or_equiv
_atom_site_occupancy
Tl1 Tl1+ a 0.6573(2) 0.02978(4) 0.82387(12) 0.0321(4) 1
. . . . .
Sb1 Sb3+ a 0.6967(4) -0.01061(6) 0.58114(17) 0.0365(7) 0.8
Pb1 Pb2+ a 0.6967(4) -0.01061(6) 0.58114(17) 0.0365(7) 0.2
Pb2 Pb2+ a 0.1897(4) -0.01719(6) 0.58657(17) 0.0403(9) 0.861(15)
. . . . .
S1 S2- a -0.0910(15) 0.9865(2) 0.9560(6) 0.031(2) 1
S2 S2- a 0.4002(11) 0.9911(2) 0.9681(6) 0.0187(17) 1

```

## 5.5 Oxidation numbers

These are looked for in either of the following parts of the CIF file:

- in the `_atom_site` section, either contained in the `_atom_site_type_symbol`, *e.g.*: Pb2+, S2- *etc.* or in a separate column corresponding to `_atom_site_oxidation_number`, *e.g.*: 2, 3, -2 *etc.*
- In a separate `loop_` elsewhere in the CIF file. Examples:

```
_atom_site_label
_atom_site_type_symbol
_atom_site_Wyckoff_symbol
_atom_site_fract_x
_atom_site_fract_y
_atom_site_fract_z
_atom_site_occupancy
Tl1 Tl1+ a 0.6573(2) 0.02978(4) 0.82387(12) 1
. . . . .
Sb1 Sb3+ a 0.6967(4) -0.01061(6) 0.58114(17) 0.8
Pb1 Pb2+ a 0.6967(4) -0.01061(6) 0.58114(17) 0.2
. . . . .
S1 S2- a -0.0910(15) 0.9865(2) 0.9560(6) 1
S2 S2- a 0.4002(11) 0.9911(2) 0.9681(6) 1
```

In this case, oxidation numbers are extracted from `_atom_site_type_symbol`. However, if the symbol does not contain the valence part, oxidation numbers must be read either from a separate column in the `_atom_site` table (see below) or from elsewhere in the CIF file:

```
_atom_site_label
_atom_site_type_symbol
_atom_site_oxidation_number
_atom_site_Wyckoff_symbol
_atom_site_fract_x
_atom_site_fract_y
_atom_site_fract_z
_atom_site_occupancy
Tl1 Tl 1 a 0.6573(2) 0.02978(4) 0.82387(12) 1
. . . . .
Sb1 Sb 3 a 0.6967(4) -0.01061(6) 0.58114(17) 0.8
Pb1 Pb 2 a 0.6967(4) -0.01061(6) 0.58114(17) 0.2
. . . . .
S1 S -2 a -0.0910(15) 0.9865(2) 0.9560(6) 1
S2 S -2 a 0.4002(11) 0.9911(2) 0.9681(6) 1
. . . . .
```

or, in the case of long lists of atoms, from a separate loop:

loop_	loop_
_atom_type_symbol	_atom_type_symbol
<b>_atom_type_oxidation_number</b>	<b>_atom_type_oxidation_number</b>
Tl1+ <b>1</b>	Tl <b>1</b>
Pb2+ <b>2</b>	Pb <b>2</b>
Sb3+ <b>3</b>	Sb <b>3</b>
S2- <b>-2</b>	S <b>-2</b>

In both cases, `_atom_type_symbol` must have an equivalent column in the `_atom_site` section flagged as `_atom_site_type_symbol`.

Any arrangements of signs, values or attached chemical symbols are acceptable as sources for oxidation numbers. However, the minus sign cannot miss in the case of anions. Monovalent cations without the actual numeric charge are also admissible (*e.g.*, Ag+).

Note: Usually, CIF files retrieved from ICSD have dedicated loops for reading the oxidation numbers. Sometimes, certain ions in the loop—known to have multiple oxidation states—are assigned with non-integer oxidation numbers despite the original papers not mentioning such values. Example:

```

loop_
_atom_type_symbol
_atom_type_oxidation_number
Ca2+ 2
Fe2+ 2.08
Al3+ 3
Si4+ 4
O2- -2

```

It may be supposed that this is done for compensating the structure-derived charge unbalances encountered in certain structures. However, it is recommended to correct such values to the formal integers. Otherwise, the program will not be able to retrieve the  $R_o$  and  $B$  values necessary for the bond valence calculation.

## 5.6 Symmetry multiplicities

ECoN21 calculates the multiplicities based on symmetry operators listed as `_symmetry_equiv_pos_as_xyz` or `_space_group_symop_operation_xyz`. If there are no symmetry operators and no multiplicities, then a value of 1 is assigned to all atoms.

## 5.7 Fractional coordinates

These are read from the `_atom_site` section:

```

_atom_site_label
_atom_site_type_symbol
_atom_site_oxidation_number
_atom_site_Wyckoff_symbol
_atom_site_fract_x
_atom_site_fract_y
_atom_site_fract_z
_atom_site_B_iso_or_equiv
_atom_site_occupancy
Tl1 Tl 1 a 0.6573(2) 0.02978(4) 0.82387(12) 0.0321(4) 1
. . . . .
Sb1 Sb 3 a 0.6967(4) -0.01061(6) 0.58114(17) 0.0365(7) 0.8
Pb1 Pb 2 a 0.6967(4) -0.01061(6) 0.58114(17) 0.0365(7) 0.2
Pb2 Pb 2 a 0.1897(4) -0.01719(6) 0.58657(17) 0.0403(9) 0.861(15)
. . . . .
S1 S -2 a -0.0910(15) 0.9865(2) 0.9560(6) 0.031(2) 1
S2 S -2 a .4002(11) .9911(2) .9681(6) 0.0187(17) 1
. . . . .

```

Leading zeros are not necessary (see the S2 line in the example above).

## 5.8 Occupancies

The program reads the occupancies from a dedicated column in the `_atom_site` section:

```

_atom_site_label
_atom_site_type_symbol
_atom_site_oxidation_number
_atom_site_Wyckoff_symbol
_atom_site_fract_x
_atom_site_fract_y
_atom_site_fract_z
_atom_site_B_iso_or_equiv
_atom_site_occupancy
Tl1 Tl 1 a 0.6573(2) 0.02978(4) 0.82387(12) 0.0321(4) 1
. . . . .
Sb1 Sb 3 a 0.6967(4) -0.01061(6) 0.58114(17) 0.0365(7) 0.8
Pb1 Pb 2 a 0.6967(4) -0.01061(6) 0.58114(17) 0.0365(7) 0.2
Pb2 Pb 2 a 0.1897(4) -0.01719(6) 0.58657(17) 0.0403(9) 0.861(15)
. . . . .
S1 S -2 a -0.0910(15) 0.9865(2) 0.9560(6) 0.031(2) 1
S2 S -2 a 0.4002(11) 0.9911(2) 0.9681(6) 0.0187(17) 1
. . . . .

```

## 5.9 Troubleshooting CIF issues

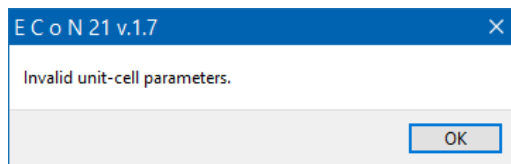
The standardization of CIF files is far from being tight and sometimes, it makes no easy task for a retrieving program to get the structure data rightly. There are many ways in which the same type of information may be written (see [Section 5.2](#) for an example) and there is no requirement that certain data which are mandatory for ECoN21 be included in the CIF file. Exotic characters such as #8217 instead of the normal single quote mark (#39) may appear in such files and there is no default mechanism to correct them (fortunately, ECoN21 does that!). Therefore, when importing a CIF file from a database or from a journal repository of supplementary materials, errors may occur.

Several of the most common syntax flaws in CIF files are observed in this section. The following fictive CIF file is taken as an example:

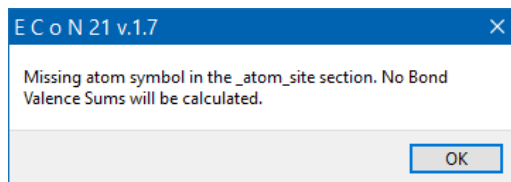
```
_cell_length_a 11.608
_cell_length_b 4.0279
_cell_length_c 11.275
_cell_angle_alpha
_cell_angle_beta
_cell_angle_gamma
_symmetry_space_group_name_H-M 'P n m a'

loop_
_atom_site_label
_atom_site_fract_x
_atom_site_fract_y
_atom_site_fract_z
Pb1 0.33320 0.25000 0.48800
Cu1 0.23200 0.25000 0.20810
Bi1 0.01850 0.25000 0.68120
S1 0.04540 0.25000 0.13730
S2 0.37950 0.25000 0.05530
S3 0.21460 0.25000 0.80360
```

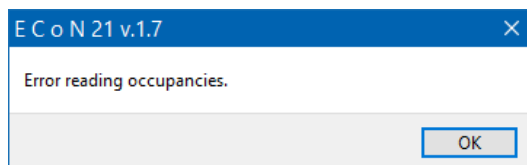
The missing alpha, beta and gamma angles will not cause any issue. When such fields are blank, the angles will be set automatically to 90 degrees. If any unit-cell parameter is wrongly recorded in the CIF file (*e.g.*, an 'O' instead of zero in 11.608), the following error message will be displayed:



On a first attempt to read the input file, the following error is generated:



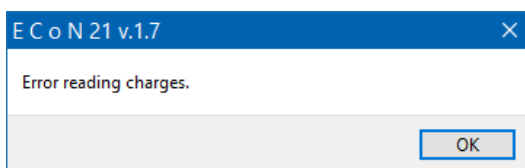
followed by:



The first error is sourced in the absence of element symbols in the `_atom_site` table, which precludes the correct display of site populations, heteroligand polyhedra content if any, and the collection of  $R_o$  and  $B$  from the list of empirical parameters. The second error is generated by the lack of occupancy values. The solution is to add the `_atom_site_type_symbol` flag and to write a column with symbols. To eliminate the second error it is necessary to add the `_atom_site_occupancy` flag and to write a column with occupancies:

```
loop_
  _atom_site_label
  _atom_site_type_symbol
  _atom_site_fract_x
  _atom_site_fract_y
  _atom_site_fract_z
  _atom_site_occupancy
Pb1  Pb  0.33320  0.25000  0.48800  1
Cu1  Cu  0.23200  0.25000  0.20810  1
Bi1  Bi  0.01850  0.25000  0.68120  1
S1   S   0.04540  0.25000  0.13730  1
S2   S   0.37950  0.25000  0.05530  1
S3   S   0.21460  0.25000  0.80360  1
```

Charges are missing from anywhere in the CIF file and therefore, the next predictable error will be



The way-out is to either add the charges to the symbol column:

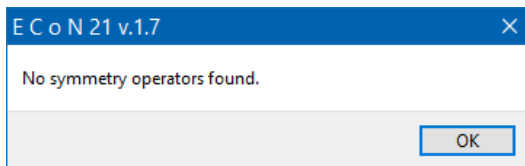
```
loop_
  _atom_site_label
  _atom_site_type_symbol
  _atom_site_fract_x
  _atom_site_fract_y
  _atom_site_fract_z
  _atom_site_U_iso_or_equiv
  _atom_site_occupancy
Pb1  Pb2+ 0.33320  0.25000  0.48800  0.03420  1
Cu1  Cu1+ 0.23200  0.25000  0.20810  0.03407  1
Bi1  Bi3+ 0.01850  0.25000  0.68120  0.01811  1
S1   S2-  0.04540  0.25000  0.13730  0.01925  1
S2   S2-  0.37950  0.25000  0.05530  0.01646  1
S3   S2-  0.21460  0.25000  0.80360  0.01064  1
```

or—in the case of very long lists of atoms—to build a new loop like so:

```
loop_
  _atom_type_symbol
  _atom_type_oxidation_number
Pb  2
Cu  1
Bi  3
S  -2
```

making sure that corresponding symbols exist in the `_atom_site` (fractional coordinates) table. Note that any lack of such correspondence (*e.g.*, symbols in the `_atom_site` table not listed in the `_atom_type_oxidation_number` loop) will generate the same error.

On a new attempt to run the file, the following error occurs:



In such cases, the symmetry operators for a given space group may be obtained either from the International Tables of Crystallography or from various web sources, *e.g.*:

- Bilbao Crystallographic Server – <https://www.cryst.ehu.es/cgi-bin/cryst/programs/nph-getgen/>
- Space Group Diagrams and Tables – <http://img.chem.ucl.ac.uk/sgp/large/sgp.htm>

In the case of the *Pnma* space group, the list of symmetry operators is:

```
'x, y, z'
'x, 1/2-y, z'
'-x, 1/2+y, -z'
'1/2-x, 1/2+y, 1/2+z'
'1/2+x, 1/2-y, 1/2-z'
'1/2+x, y, 1/2-z'
'1/2-x, -y, 1/2+z'
'-x, -y, -z'
```

This list must be placed in a separate loop following any of the syntaxes described in [Section 5.2](#). Finally, the CIF file will be read adequately and the calculation can proceed.

Note however, that some crystal structures are not completely solvable by ECoN21 even if the CIF files are complete and correct. Often, such problematic cases are represented by structures containing more than two (partially occupied) central atom or ligand positions which occur very close to each other (multiple split positions). Such a distribution of atoms prevents the correct determination of CP faces, volumes, centroids or derived quantities, and are also likely to yield erratic CD and BVS results.

Example: makovickyite (Nakashima *et al.*, 2013): the octahedra connecting pairs of Bi square pyramids in the thin layer of the structure are populated by 6 partially occupied Cu in eccentric positions ([Figure 12](#)) which prove very difficult to manage in anion-centered description, both in CD and **Coordination geometry** calculations.

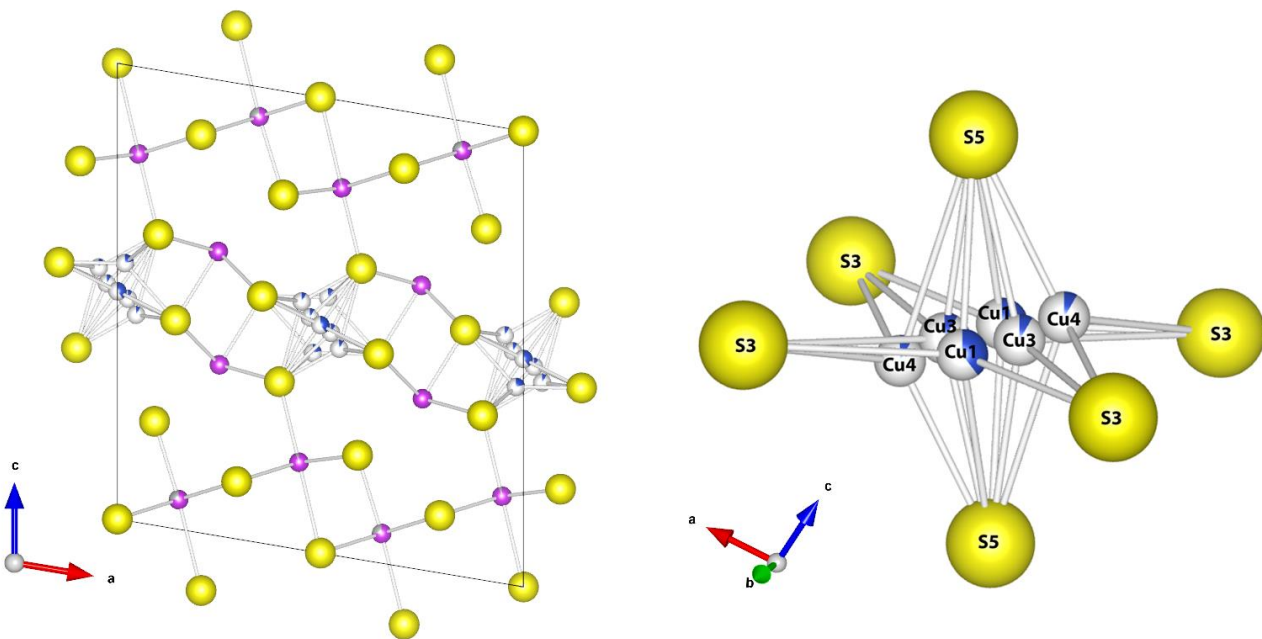


**Figure 12.** The crystal structure of makovickyite (Nakashima *et al.*, 2013) with multiple partially occupied Cu positions inside the octahedral cage connecting pairs of Bi square pyramids in the thin layer of the structure. Purple color marks Bi and Bi-Ag atoms.

Given the high number of copper atoms inside the octahedron, a number of false polyhedral faces occur during the computation. Also the *MAPD* for ligands in the anion-centered CD calculation exceeds 38% and should be taken with caution.

Minerals of the pearceite group are roughly in the same category. For example, in Se-rich antimonpearceite (Evain *et al.*, 2006), part of Ag is distributed along two-dimensional diffusion paths shaped as hexagonal-like loops (Figure 13). Maxima of electron density along these paths do not correspond to the refined Ag position and do not reflect in meaningful distances.

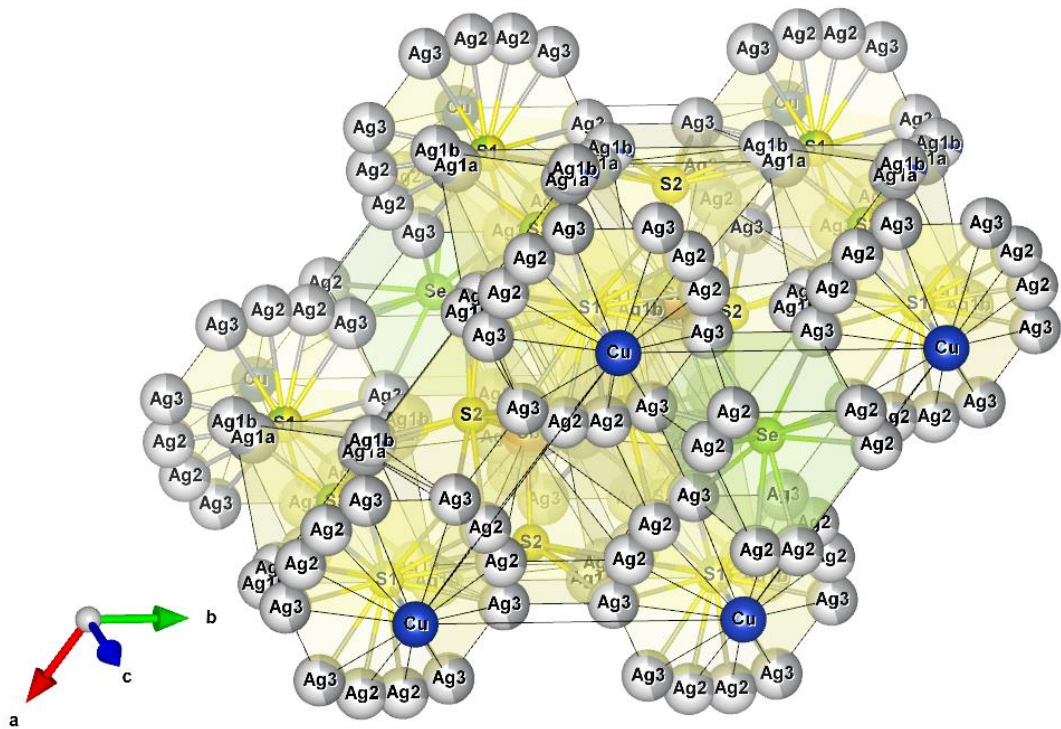


**Figure 13.** The crystal structure of Se-rich antimonpearceite (Evain *et al.*, 2006) with multiple partially occupied Ag positions delineating hexagonal-like diffusion paths, *i.e.*, quasi-continuous areas of elevated electron density. Another example of crystal structure not really solvable by ECoN21.

Also note that some errors will not be parsed by the program. One of the most common error occurs when the text editor word wrapping is checked on and the text which should appear in a single line is divided among two lines:

```
Ba Ba 0.34788(2) 0.28063(2) -0.12996(6) 0.00695(8) Uani d . . . 1 . .
Nb Nb 0.22256(2) 0.38075(2) 0.37325(10) 0.00842(11) Uani d . P . 0.8241 .
.
Fe Fe2 0.22256(2) 0.38075(2) 0.37325(10) 0.00842(11) Uani d . P . 0.1759 .
.
Fe Fe3 0.21260(4) 0.39221(4) 0.86873(17) 0.00398(15) Uani d . P . 0.2175 .
.
```





## 6 The $R_o$ and $B$ parameters

ECoN21 attempts to extract the  $R_o$  and  $B$  values automatically from the *bvsparm.cif* file which should exist in the same folder as the main executable file. The *bvsparm.cif* file is a slightly modified version of the *bvparm2020.cif* file (Brown, 2020) issued by IUCr. Because the original file sometimes contained multiple parameters for a specific pair of atoms, these were reordered by putting the preferred values on the first position in the list of duplicates. Such values are supposed to be the first matches during the search for  $R_o$  and  $B$  parameters, and were chosen mainly on the basis of their more recent publication date and how much the author of this list trusted certain sources. The user may decide upon different priorities among these groups of multiple values.

Below is a fragment of this file showing pairs of cations and anions of certain valences, the  $R_o$  and  $B$  parameters, a pointer to a reference list, and a column for comments. A question mark indicates that no comments were due.

```

loop_
  _valence_param_atom_1
  _valence_param_atom_1_valence
  _valence_param_atom_2
  _valence_param_atom_2_valence
  _valence_param_Ro
  _valence_param_B
  _valence_param_ref_id
  _valence_param_details

Ac 3   O  -2   2.24   0.37   b  ?
Ac 3   O  -2   2.29   0.35   p  ?
Ac 3   F  -1   2.13   0.37   b  ?
Ac 3   F  -1   2.10   0.40   p  ?
Ac 3  Cl -1   2.63   0.37   b  ?
Ac 3  Cl -1   2.60   0.40   p  ?
Ac 3  Br -1   2.75   0.40   p  ?
Ag 1   O  -2   1.842  0.37   a  ?
Ag 1   O  -2   1.875  0.359  bs ?
Ag 1   O  -2   1.805  0.37   b  ?
Ag 1   S  -2   2.119  0.37   a  ?
Ag 1   F  -1   1.80   0.37   b  ?
Ag 1  Cl -1   2.09   0.37   b  ?
Ag 2   F  -1   1.79   0.37   e  unchecked
Ag 3   F  -1   1.83   0.37   e  unchecked
Ag 9  Br -1   2.22   0.37   b  ?
Ag 9   I  -1   2.38   0.37   b  ?
Ag 9  Se -2   2.26   0.37   b  ?
Ag 9  Te -2   2.51   0.37   b  ?
Ag 9   N  -3   1.85   0.37   b  ?
Ag 9   P  -3   2.22   0.37   b  ?
Ag 9  As -3   2.30   0.37   b  ?
Ag 9   H  -1   1.50   0.37   b  ?
Al 3   O  -2   1.651  0.37   a  ?
Al 3   O  -2   1.634  0.390  bs ?
Al 3   O  -2   1.644  0.38   o  ?
Al 3   S  -2   2.13   0.37   b  ?
Al 3   S  -2   2.21   0.37   e  unchecked
Al 3  Se -2   2.27   0.37   b  ?
Al 3  Te -2   2.48   0.37   b  ?
Al 3   F  -1   1.545  0.37   a  ?
Al 3  Cl -1   2.032  0.37   a  ?
Al 3  Br -1   2.20   0.37   b  ?
Al 3   I  -1   2.41   0.37   b  ?
Al 3   N  -3   1.79   0.37   b  ?
Al 3   P  -3   2.24   0.37   b  ?
Al 3  As -3   2.30   0.37   b  ?
Al 3   H  -1   1.45   0.37   b  ?
Am 3   O  -2   2.11   0.37   b  ?
. . . . .

```

As shown in the example above, in order to find the relevant parameters for a certain bond, the search routine must be aware of the chemical symbols and the oxidation numbers of the atoms in question. This is only possible if:

- a) the **\_atom\_site** section contains valid atom symbols such as Pb2+, Sb3+, S2-, from where both the chemical symbol and the oxidation number can be extracted.
- b) the **\_atom\_site** section contains valid atom symbols such as Pb, Sb, S and the CIF file contains a separate list wherefrom the corresponding oxidation numbers can be extracted.

Note that in order to perform the automated BVS calculation, the program needs to find *all* the  $R_o$  and  $B$  pairs required for a CP. If any pair of parameters is missing for a given bond, then no BVS calculation will take place for that CP.

Once a new version of the *bvparm2020.cif* file is released by IUCr, it can be copied into the main executable file's folder and renamed '*bvsparm.cif*' in order to be recognized by the program.

## 7 Dealing with hydrogen atoms and bonds

One of the difficult issues of crystal structure determination concerns hydrogen atoms and bonds. On the one hand, hydrogen positions are difficult to obtain and often the accuracy of their fractional coordinates is low. On the other hand, hydrogen has a peculiar behavior in terms of charge distribution, requiring a much lower exponent factor in [Equations \(2\), \(3\) and \(4\)](#) (see [Section 2.1](#)). Under normal circumstances, using the constraint factor established by Nespolo *et al.* (2001), the calculation should be straightforward as in the example given further on (ICSD 184708—gibbsite  $\text{Al}(\text{OH})_3$  and references therein); only the relevant lines and values are given in the example):

```
_chemical_formula_structural 'Al (O H)3'
_cell_length_a 8.684(1)
_cell_length_b 5.078(1)
_cell_length_c 9.736(2)
_cell_angle_alpha 90.
_cell_angle_beta 94.54(1)
_cell_angle_gamma 90.
_space_group_name_H-M_alt 'P 1 21/n 1'
loop_
_space_group_symop_id
_space_group_symop_operation_xyz
1 '-x+1/2, y+1/2, -z+1/2'
2 '-x, -y, -z'
3 'x+1/2, -y+1/2, z+1/2'
4 'x, y, z'
loop_
_atom_type_symbol
_atom_type_oxidation_number
Al3+ 3
O2- -2
H1+ 1
loop_
_atom_site_label
_atom_site_type_symbol
_atom_site_fract_x
_atom_site_fract_y
_atom_site_fract_z
_atom_site_occupancy
Al1 Al3+ 0.1679(1) 0.5295(2) -0.0023(1) 1
Al2 Al3+ 0.3344(1) 0.0236(2) -0.0024(4) 1
O1 O2- 0.1779(2) 0.2183(4) -0.1115(2) 1
O2 O2- 0.6692(2) 0.6558(4) -0.1023(2) 1
O3 O2- 0.4984(2) 0.1315(4) -0.1044(2) 1
O4 O2- -0.0205(2) 0.6293(4) -0.1068(2) 1
O5 O2- 0.2971(2) 0.7178(4) -0.1052(2) 1
O6 O2- 0.8194(2) 0.1491(4) -0.1015(2) 1
H1 H1+ 0.101(6) 0.152(10) -0.124(5) 1
H2 H1+ 0.595(6) 0.573(10) -0.098(5) 1
H3 H1+ 0.503(5) 0.137(10) -0.190(5) 1
H4 H1+ -0.029(5) 0.801(10) -0.107(4) 1
H5 H1+ 0.293(6) 0.724(11) -0.196(6) 1
H6 H1+ 0.815(5) 0.160(9) -0.190(5) 1
```

Results of ECoN21 calculation (summary):

Cation	CN	ECoN	qX	QX	qX/QX	BVS	$\Delta R(\text{Ba})$	$\Delta R(\text{Br})$
Al1	6	5.941	3.000	3.019	0.994	3.055	0.012	0.001
Al2	6	5.951	3.000	2.968	1.011	3.028	0.015	0.001
H1	1	1.000	1.000	1.027	0.974	1.485	0.000	0.000
H2	1	1.000	1.000	1.031	0.970	1.403	0.000	0.000
H3	1	1.000	1.000	0.970	1.031	1.206	0.000	0.000
H4	1	1.000	1.000	1.022	0.979	1.106	0.000	0.000
H5	1	1.000	1.000	0.916	1.091	1.087	0.000	0.000
H6	1	1.000	1.000	1.048	0.954	1.142	0.000	0.000
-----								
MAPD: 3.23%			18.21%		<0.003>		<0.000>	

Anion	qA	QA	qA/QA	BVS	$\Delta R(\text{Ba})$	$\Delta R(\text{Br})$
O1	-2.000	-1.948	1.027	2.452	0.340	0.059
O2	-2.000	-1.940	1.031	2.364	0.332	0.054
O3	-2.000	-2.063	0.970	2.268	0.303	0.031
O4	-2.000	-1.958	1.022	2.085	0.295	0.031
O5	-2.000	-2.183	0.916	2.266	0.281	0.017
O6	-2.000	-1.909	1.048	2.077	0.302	0.037
-----						
MAPD: 4.09%		12.60%		<0.309>		<0.038>

In certain CIF files, the OH<sup>-</sup> group is localized only by means of oxygen atoms, with no hydrogen coordinates determined whatsoever, as in the next example of the same mineral gibbsite Al(OH)<sub>3</sub> (ICSD 27698—and references therein—fragment):

```

_chemical_formula_structural 'Al (O H)3'
_chemical_name_mineral Gibbsite
_cell_length_a 8.676(2)
_cell_length_b 5.070(2)
_cell_length_c 9.721(3)
_cell_angle_alpha 90.
_cell_angle_beta 94.57(8)
_cell_angle_gamma 90.
_space_group_name_H-M_alt 'P 1 21/n 1'
loop_
_space_group_symop_id
_space_group_symop_operation_xyz
1 '-x+1/2, y+1/2, -z+1/2'
2 '-x, -y, -z'
3 'x+1/2, -y+1/2, z+1/2'
4 'x, y, z'
loop_
_atom_type_symbol
_atom_type_oxidation_number
O2- -2
Al3+ 3
loop_
_atom_site_label
_atom_site_type_symbol
_atom_site_fract_x
_atom_site_fract_y
_atom_site_fract_z
_atom_site_occupancy
O1 O2- 0.183 0.202 -0.105 1
O2 O2- 0.674 0.670 -0.104 1
O3 O2- 0.480 0.132 -0.106 1
O4 O2- -0.017 0.632 -0.108 1
O5 O2- 0.293 0.702 -0.105 1
O6 O2- 0.806 0.170 -0.103 1
Al1 Al3+ 0.166 0.500 0.000 1
Al2 Al3+ 0.333 0.000 0.000 1

```

Running the CIF file as it is, would yield a huge charge unbalance and overall wrong results:

Cation	CN	ECoN	qX	QX	qX/QX	BVS	ΔR (Ba)	ΔR (Br)
Al1	13	5.878	3.000	6.019	0.498	3.225	0.518	0.678
Al2	13	5.824	3.000	5.981	0.502	3.229	0.521	0.682
MAPD: 100.00%						7.56%	<0.519>	<0.680>
Anion	qA	QA	qA/QA	BVS	ΔR (Ba)	ΔR (Br)		
O1	-2.000	-1.078	1.855	1.140	0.489	0.644		
O2	-2.000	-0.927	2.159	1.012	0.449	0.585		
O3	-2.000	-0.967	2.068	1.054	0.593	0.770		
O4	-2.000	-0.952	2.101	1.035	0.585	0.762		
O5	-2.000	-1.109	1.803	1.166	0.496	0.660		
O6	-2.000	-0.967	2.068	1.048	0.458	0.592		
MAPD: 50.00%				46.22%	<0.156>	<0.205>		

Instead, the charge of the oxygen atoms should be modified manually to  $-1$ , that is, to the charge of the  $\text{OH}^-$  group, keeping in mind that  $\text{O}^{2-}$  is in fact  $\text{OH}^-$ :

```
_atom_type_symbol
_atom_type_oxidation_number
Al3+ 3
O2- -1
```

Or, for a more conformable output, by manually editing the CIF file as follows: the `_atom_type_symbol` and `_atom_site_type_symbol` for oxygen should be modified to  $\text{OH}^-$  and the charge set to  $-1$ . The atom labels should also be changed, accordingly:

```
_atom_type_symbol
_atom_type_oxidation_number
Al3+ 3
OH- -1
loop_
_atom_site_label
_atom_site_type_symbol
_atom_site_fract_x
_atom_site_fract_y
_atom_site_fract_z
_atom_site_occupancy
OH1 OH1- 0.183 0.202 -0.105 1
OH2 OH1- 0.674 0.670 -0.104 1
OH3 OH1- 0.480 0.132 -0.106 1
OH4 OH1- -0.017 0.632 -0.108 1
OH5 OH1- 0.293 0.702 -0.105 1
OH6 OH1- 0.806 0.170 -0.103 1
Al1 Al3+ 0.166 0.500 0.000 1
Al2 Al3+ 0.333 0.000 0.000 1
```

The results for this new input will be considerably better, however, at the expense of BVS results which will not be available any longer (no empirical parameters for  $\text{Al}^{3+}-\text{O}^-$  or  $\text{Al}^{3+}-\text{OH}^-$  bonds are contained in the *bvsparm.cif* file):

Cation	CN	ECoN	qX	QX	qX/QX	BVS	ΔR (Ba)	ΔR (Br)
Al1	13	5.878	3.000	3.009	0.997	-	0.518	-
Al2	13	5.824	3.000	2.991	1.003	-	0.521	-
MAPD: 0.31%						n/a	<0.519>	< n/a >
Anion	qA	QA	qA/QA	BVS	ΔR (Ba)	ΔR (Br)		
OH1	-1.000	-1.078	0.927	-	0.489	-		
OH2	-1.000	-0.927	1.079	-	0.449	-		
OH3	-1.000	-0.967	1.034	-	0.593	-		
OH4	-1.000	-0.952	1.050	-	0.585	-		
OH5	-1.000	-1.109	0.902	-	0.496	-		
OH6	-1.000	-0.967	1.034	-	0.458	-		
MAPD: 6.25%				n/a	<0.156>	< n/a >		

## 8 Opposing bond lengths—the Trömel diagram

This part of the Coordination Geometry calculation identifies the 'in plane' and 'out of plane' pairs of opposing bond lengths found in *distorted* coordination octahedra and monocapped trigonal prisms. Such pairs of distances are plotted in the XY diagrams described by Trömel (1980) and Berlepsch *et al.* (2001a, 2001b) and are used to distinguish mixed sites from pure ones or to check upon the correct assignment of a chemical type to a given atom position. The method is based on the tendency of  $x_n y_n$  bond distance pairs to plot along element specific hyperbolae which comply with the rule:

$$(x - h)(y - h) = c \quad (c > 0)$$

where  $h$  and  $c$  are element specific parameters.

### 8.1 Definition of 'in plane' and 'out of plane' bond pairs

In distorted coordination octahedra, the 'plane' referenced by the 'in plane' and 'out of plane' concepts, is defined by the ligands forming the common base of the square pyramids. In monocapped trigonal prisms, the 'plane' is determined by the base of the capping pyramid. The  $x_i$  bonds belonging to a 'in plane' set of bonds represent the stronger interactions (*i.e.*, the shorter distances), whereas the  $y_i$  bonds represent the weaker (*i.e.*, longer) ones. The 'out of plane' bonds develop approximately normal to the 'planes', but the designation of weaker and stronger interactions is reversed:  $x_o$  represent the longer bond of the pair and  $y_o$  the shorter one. In CP of metals with high lone electron pair (LEP) activity,  $x_o$  corresponds to the direction of LEP. In octahedral coordinations, beside two pairs of 'in plane' bonds (*i.e.*,  $x_1 y_1, x_2 y_2$  in Figure 14a) there is one pair of 'out of plane' ones ( $x_o y_o$  in the same figure). However, in monocapped trigonal prisms (Figure 14b) the 'out of plane' bonds form two pairs, *i.e.*,  $x_o y_o$  and  $x_o^* y_o$ . The literature (*e.g.*, Berlepsch *et al.* 2001a, 2001b) indicates that only one of these pairs is used for the actual plots in hyperbolic diagrams. Choosing one pair or another relies either on the bond angles of  $x_o y_o$  and  $x_o^* y_o$  (*e.g.*, the choice is made for the pair with larger bond angle), the shortest  $x_o$  distance or on keeping a consistent orientation of the  $x_o$  bonds throughout the structure. The program calculates both pairs, letting the user to interpret and choose what to plot. A visual definition of the 'in plane' and 'out of plane' bond pairs is shown in Figure 14.

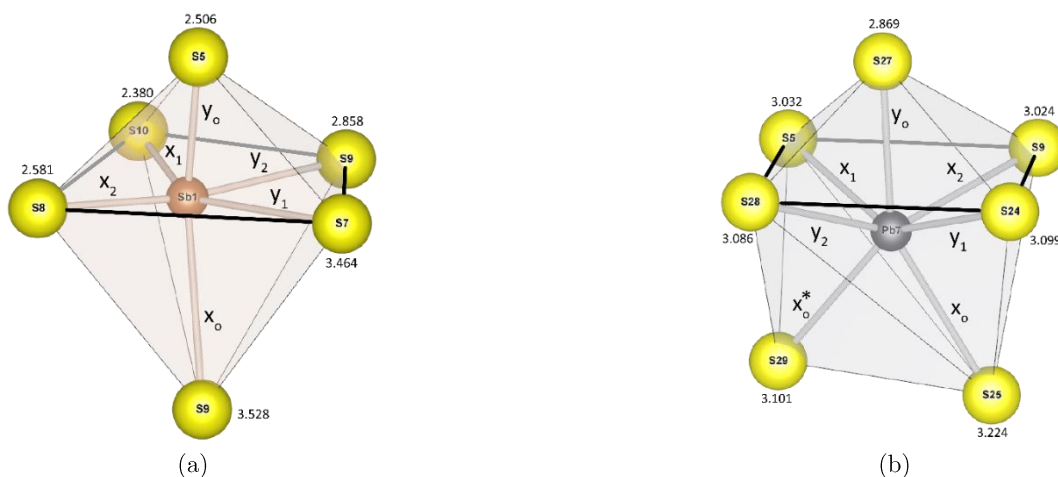


**Figure 14.** Examples of 'in plane' and 'out of plane' opposing bond pairs in a distorted coordination octahedron (a) and a monocapped trigonal prism (b). In both cases, the actual 'plane' is marked with thicker line. For the 'in plane' bond pairs,  $x_i$  are shorter than  $y_i$ , whereas for the 'out of plane' ones,  $x_o$  are chosen to be longer than  $y_o$ . The  $x_o^*$  symbol denotes a second connection opposed to the capped face which—for example—has a smaller S-Me-S bond angle.

The concept of 'in-plane' and 'out of plane' depends on the overall texture of the atomic arrangement. The crystal structure has to contain rows, ribbons, double-ribbons, planes or rods based on ribbon-like organization, with low periodicity in one direction (about 4 Å or 8 Å), and furthermore, with well-developed LEP spaces. In a structure with a common LEP micelle formed by several neighbors ([Figure 15](#)), the concept is easiest to define: their common plane defines the 'in-plane' vectors and the distances normal to them are 'out of plane' (Emil Makovicky, personal communication). In such situations, the program is able to automatically identify the vector (*i.e.*, the zone axis) of the 'in-plane' configurations as long as the ☒ **Auto detect** option is checked in the [Calculation Settings](#) dialog.

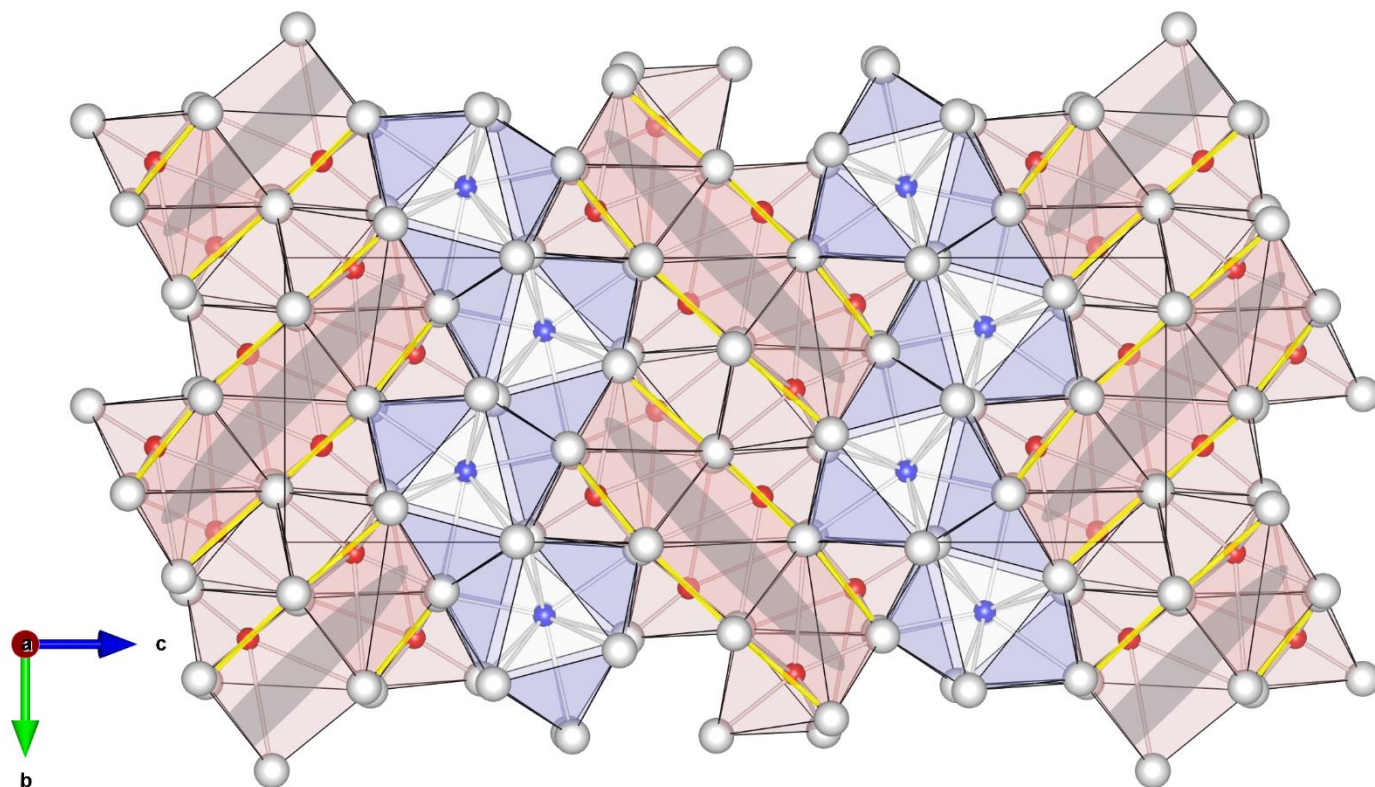


**Figure 15.** Generic crystal structure derived from rathite (Berlepsch *et al.*, 2002) with some CP and split positions omitted for clarity. The structure shows 'standing' tricapped trigonal prisms (blue) and 'lying' monocapped prisms (red). The 'planes' referenced by the 'in plane' and 'out of plane' notions are marked with yellow thick lines. In this case, all 'planes' belong to the [100] zone axis. Gray ellipses delineate LEP planes. Small spheres are metal atoms and the large white ones, sulfur.

There are cases of CP with shapes far from octahedral or other simple-definable forms, and the LEP-active elements dispersed among them, for which the concept becomes ambiguous—with possible 'in plane' and 'out of plane' existing in several orientations. For such situations, the [uvw] vector of the 'plane' must be indicated by the user after checking the ☒ **Specify zone axis** control in the [Calculation Settings](#) dialog.

## 8.2 Bond-length ratio hyperbolae

Several characteristic hyperbolae have been defined for Sb-O, Te-O, I-O (Trömel, 1980) Pb-S, Bi-S, Sb-S, As-S and Sn-S bonds (Berlepsch *et al.*, 2001a, 2001b, Sejkora *et al.*, 2003, Topa, 2001, Topa *et al.*, 2003). The Me-S hyperbolae are included in the *OpposingBonds.xlsx*—a MS Excel template file which accompanies the program, and which can be used for plotting of values calculated with ECoN21 ([Figure 16](#)).

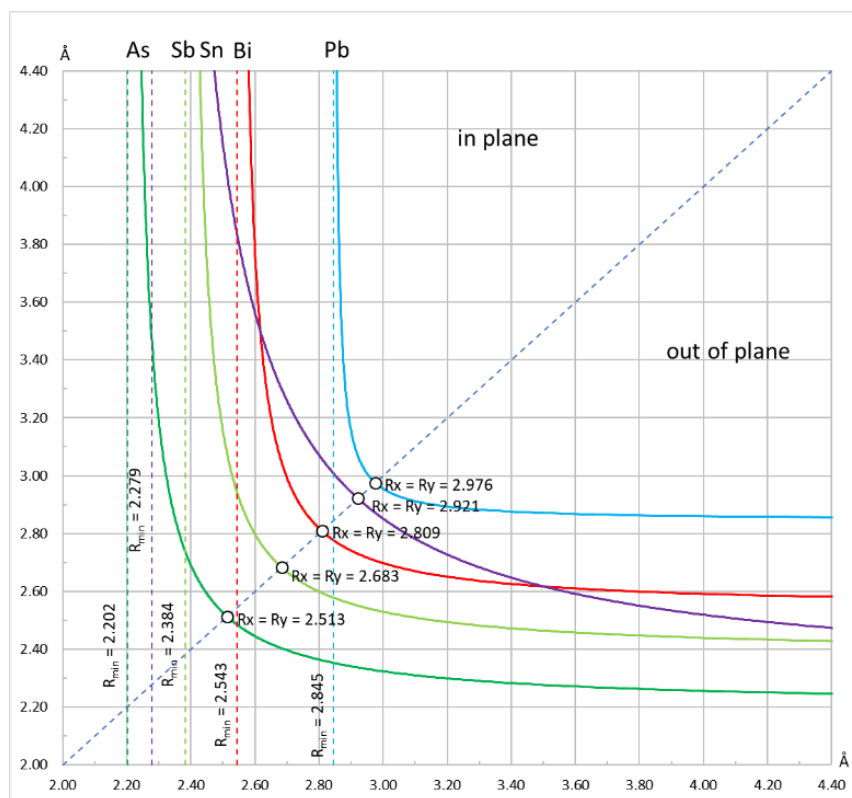


**Figure 16.** Element characteristic hyperbolae for Pb-S, Bi-S, Sb-S, As-S and Sn-S contained in the *OpposingBonds.xlsx* file and which can be used to plot opposing bonds pairs calculated by the program.

The  $h$  and  $c$  parameters used for each of the calibrated hyperbolae are given in [Table 2](#).

**Table 2.** Constants  $h$  and  $c$  used for element specific hyperbolae represented in [Figure 16](#) and included in the *OpposingBonds.xlsx* file. The  $h$  parameter represents the abscissa of the asymptote to a given hyperbola and  $R_{x=y}$  the point of equal opposing distances.

Atom	$h$ (Å)	$c$ (Å)	$R_{x=y}$ (Å)	Reference
As	2.202	0.097	2.513	Berlepsch <i>et al.</i> , 2001b
Sb	2.384	0.0895	2.683	Berlepsch <i>et al.</i> , 2001b
Bi	2.543	0.707	2.809	Topa <i>et al.</i> , 2003
Sn	2.279	0.413	2.922	Sejkora <i>et al.</i> , 2003
Pb	2.845	0.017	2.976	Topa, 2001

The Excel file contains a template table for transferring the data produced by the program. The table has dedicated columns for various types of atoms which will be plotted with distinctive symbols and colors in the final diagram.

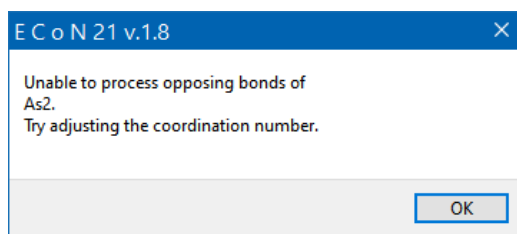
The narrow availability of calibrated hyperbolae limits the scope of this calculation to Pb, Sn, Bi, As, Sb sulfosalts. However, the calculation can be used to collect data for refining other hyperbolae. Unless used for plotting bond-length pairs against available element-specific or for constructing new hyperbolae, the calculation of opposing bond pairs has little relevance. However, the user may choose to discard this calculation altogether by checking off the ☒ **Opposing bonds** box in the [Calculation settings](#) dialog. Please note that the calculation of opposite bonds is not carried out in the anion-centered description.



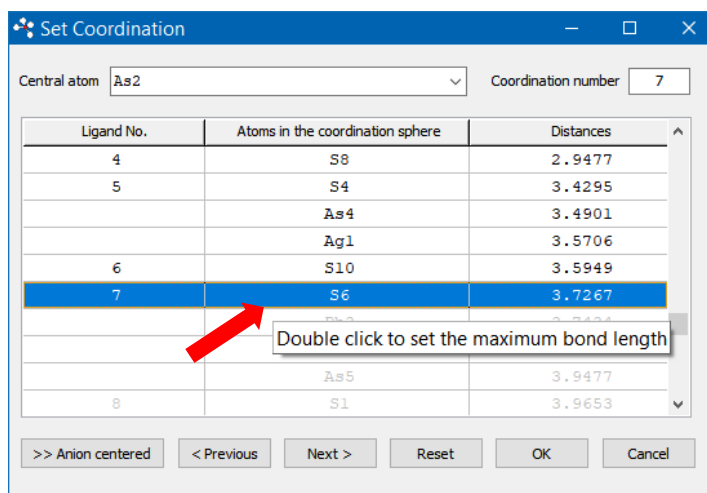
The interpretation of the plots is made in terms of site population with either pure or mixed metals. Ideally, for pure metal sites, both the 'in plane' and 'out of plane' pairs should plot on or close to the corresponding hyperbola. Mixed (binary) sites should plot between the corresponding hyperbolae.

### 8.3 Step-by-step calculation example

1. Consider the structure of rathite –  $\text{Pb}_8\text{Pb}_{4-x}(\text{Tl}_2\text{As}_2)_x(\text{Ag}_2\text{As}_2)\text{As}_{16}\text{S}_{40}$ ,  $P21/c$  (Berlepsch *et al.* 2002). Open the *rathite.cif* file which is included in the examples packed with the program. Make sure that the ☒ Opposing bonds box in the **Calculation settings** dialog, is checked on.
2. Press **Calculate** to run a first calculation using the default coordination radius threshold of 4 Å and then press **Coordination geometry**. For this radius, certain cations that show a tendency to form short bonds (*e.g.*, As) will not produce proper opposite bond pairs and the program will generate a message of the following type:



3. In this case, either check the ☒ Calculate for CN=6 or 7 only control in the **Calculation settings** dialog to ignore such deviating CP altogether or use the **Bond-type specific thresholds** or the **Polyhedron specific thresholds** to adjust the CN for the problematic atoms. The list of positions with unprocessed opposing bonds is displayed in the lower part of the dialog. For instance, in the given example, As2 will result with CN=8, but with a polyhedral shape that cannot be processed for opposing bonds (*i.e.*, not in the shape of a bicapped trigonal prism: **Figure 18a**). In the **Calculation settings** dialog, check the **Polyhedron specific thresholds** radio button to open the **Set Coordination** dialog. Use the **Central atom** drop list and navigate to As2 as in the figure below.



A double click on S6 will reduce the CN to 7 (**Figure 18b**). S10 might be double clicked as well to limit the CN to 6 (**Figure 18c**). In both cases, the program will be able to establish the 'in plane' and the 'out of plane' opposing bonds. If there are no such troublesome atoms, then jump to step 5.

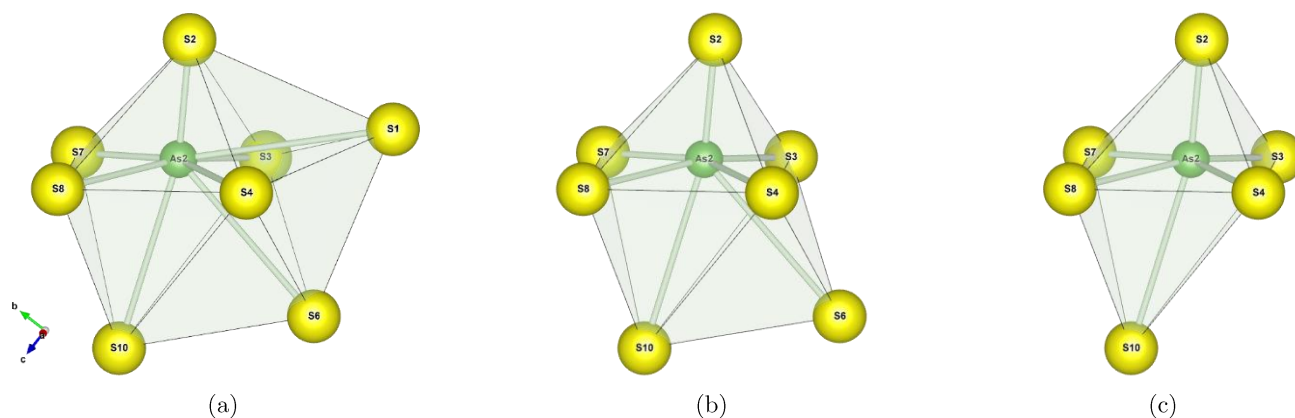


**Figure 18.** (a) The CP found by ECoN21 for As<sub>2</sub> at a global coordination radius of 4 Å (CN=8) and which cannot be processed for opposing bonds. Reducing the coordination radius will yield CP with CN=7 (b) or CN=6 (c) that will allow the proper designation of 'in plane' and 'out of plane' bond pairs.

4. After closing the **Calculation settings** dialog press **Calculate** and **Coordination geometry** again.
5. Switch to **Detailed results** ☒ view and navigate to the **Opposing Bonds** listing. Check whether everything is alright and then choose **Save as...**. In the **Save As...** dialog choose **Save as type** 'ECoN21 opposing bonds (\*.csv)'. In Explorer, open the destination folder and double-click the saved CSV file.
6. The file will open in MS Excel. Delete the opposing bond pairs to be excluded from plotting.
7. Open the *OpposingBonds.xlsx* template provided with ECoN21 package and select the **Data** sheet.
8. Transfer (copy/paste) data (**Atom Label**, **RX**, **RY** and optionally the **Angle** and 'in plane'/'out of plane' columns) from the CSV file to the **Data** sheet.
9. Open the **Diagram** sheet. The data should appear in the hyperbolic diagram (**Figure 19**). The Pb bond pairs deviating from the hyperbola belong to 'standing' tricapped prisms which do not comply with the conditions described in **Section 8.1**.

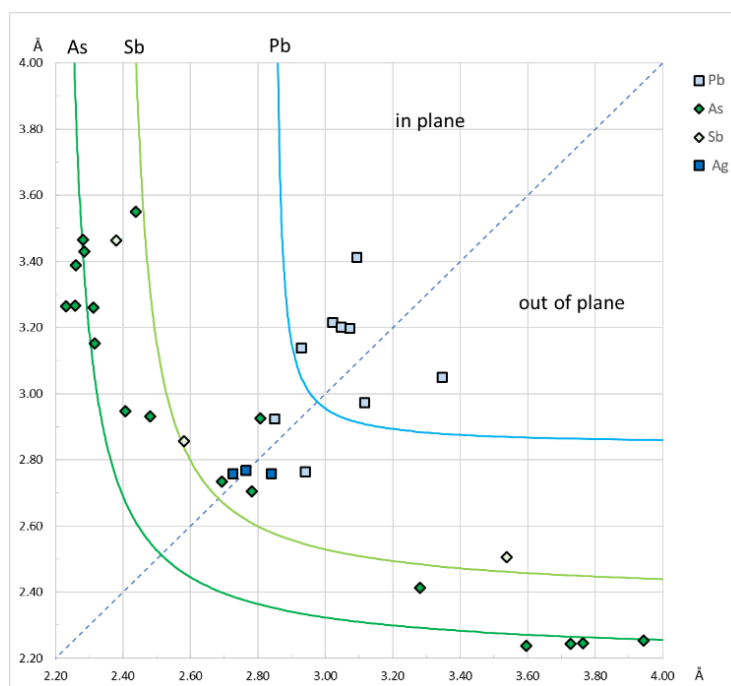


**Figure 19.** The bond-length ratio hyperbolae with 'in plane' and 'out of plane' bond pairs generated with ECoN21 for rathite (Berlepsch *et al.*, 2002).

### 8.4 Opposing bond pairs and the coordination number

The use of 'in plane' and 'out of plane' bond pairs requires a minimum CN of 6, regardless of how this number is determined by the charge distribution, bond valence sum or by the general behavior of a given metal (*e.g.*, in general, As forms three short bonds with S while the rest of the distances up to CN=6 are long and with practically zero charge exchange). Therefore, the more or less arbitrary settings such as **Maximum coordination radius**, **Bond-type specific threshold** or **Polyhedron specific threshold** must be used to adjust the CN and to obtain relevant pairs of opposing bonds. Ultimately, two pairs of 'in plane' bonds and one pair of 'out of plane' bonds end up being plotted in the diagram. Therefore, at least for the purpose of identifying opposite bond pairs, and whenever possible, the CN should be set to 6 or 7 for all CP of interest. By checking the ☒ **Calculate for CN=6 or 7 only** in the **Calculation Settings** dialog, the program may be set to calculate the opposing bonds only for octahedra or monocapped prisms.

The arbitrary choice of one set of 'in plane' and 'out of plane' in bi- or tricapped trigonal prisms (*i.e.*, CN=8 and CN=9, respectively) may not always lead to the best solution. Consider the following example of a Sb position which—at a coordination radius threshold of 4 Å—forms a bicapped trigonal prism (CN=8) with the following sets of opposing bonds:

Central atom		RX	RY	Angle		Opposing ligands	
Sb13	Set1	2.461	3.560	165.75	in plane	S38	S13
		2.396	3.339	152.81	in plane	S37	S14
		3.978	2.529	139.18	out of plane	S21	S20
		3.612	2.529	127.31	out of plane*	S22	S20
	Set2	2.396	3.612	145.23	in plane	S37	S22
		2.461	3.978	127.65	in plane	S38	S21
		3.339	3.009	126.01	out of plane	S14	S39
		3.560	3.009	114.75	out of plane*	S13	S39

These sets are illustrated in **Figure 20**.

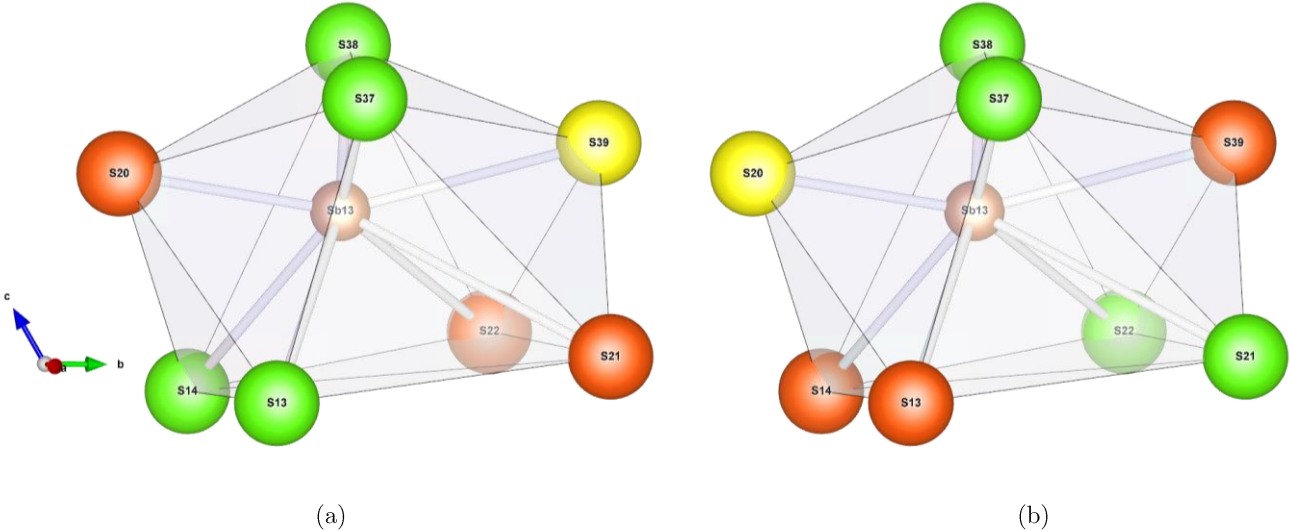


**Figure 20.** Set 1 (a) and Set 2 (b) of 'in plane' and 'out of plane' bond pairs for the generic Sb position at CN=8. The 'in plane' bond pairs are rendered in green, and the 'out of plane' ones, in red.

By excluding the two longest bonds, the CN is reduced to 6 as in **Figure 21**. We will call this Set 3:

Central atom		RX	RY	Angle		Opposing ligands	
Sb13	Set 3	2.461	3.560	165.75	in plane	S38	S13
		2.396	3.339	152.81	in plane	S37	S14
		3.009	2.529	155.89	out of plane	S39	S20

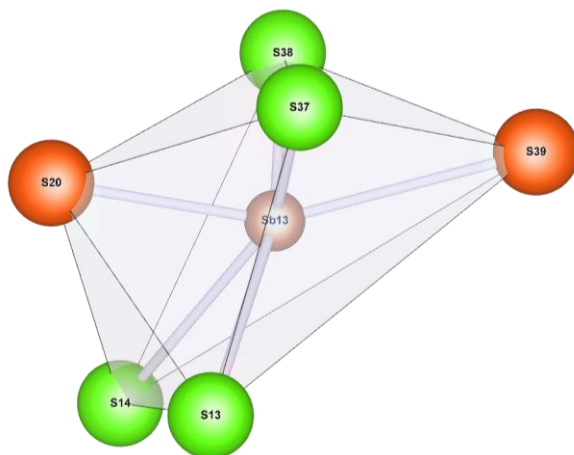


**Figure 21.** The Set 3 defined for CN=6 with two pairs of 'in plane' bonds similar to those in Set 1, and one pair of 'out of plane' bonds: S39-S20.

The first two sets plot as in [Figure 22](#), with the 'out of plane' bond pairs of Set 2 deviating considerably from the Sb hyperbola. Set 1 plots closer to the Sb curve, but still in the interspace separating Sb and Pb hyperbolae. In turn, the 'out of plane' pair of Set 3—defined for CN=6—plots right on the hyperbola, thus suggesting a pure Sb position.

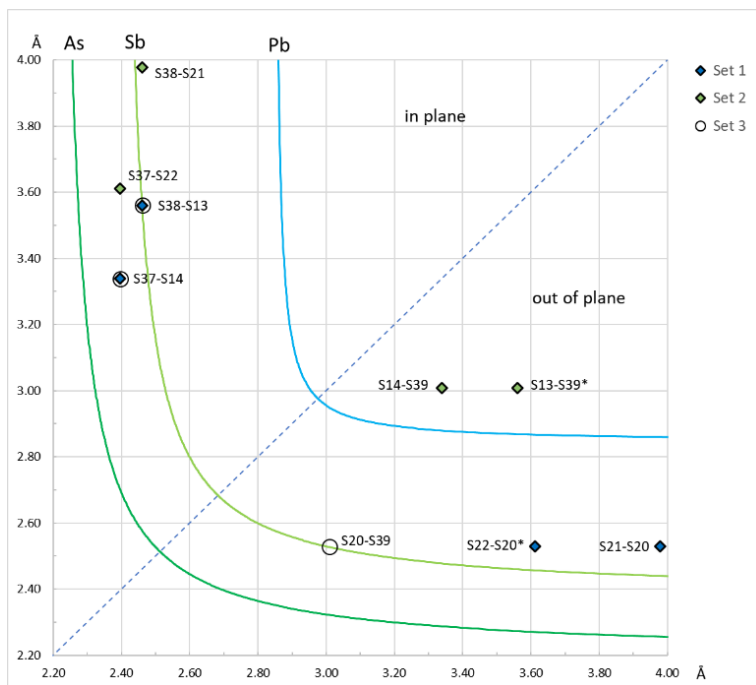


**Figure 22.** The plots of Set 1 and Set 2 for the eight-fold coordinated Sb13 position. The 'out of plane' pairs of Set 2 deviate considerably from the Sb hyperbola. Best results are obtained for Set 3 which contains opposing bond pairs defined for CN=6.

## 9 The Armbruster-Hummel diagram

In 1987, Armbruster and Hummel published a simple discriminatory diagram where the average distance of the three shortest Me-S bonds is plotted against the average of the fourth and fifth shortest distances in a given CP. The calculation of such '123/45' averages may be carried out by the program if the ☒ '123/45' averages control in the [Calculation Settings](#) dialog is checked on. The diagram allows the separation of As, Sb, Bi, Pb and Tl which plot in specific fields as represented in [Figure 23](#). The element-specific fields were outlined based on a selection of over 1600 CP in sulfosalt structures, which is considerably larger than the one used in the original paper of Armbruster and Hummel.

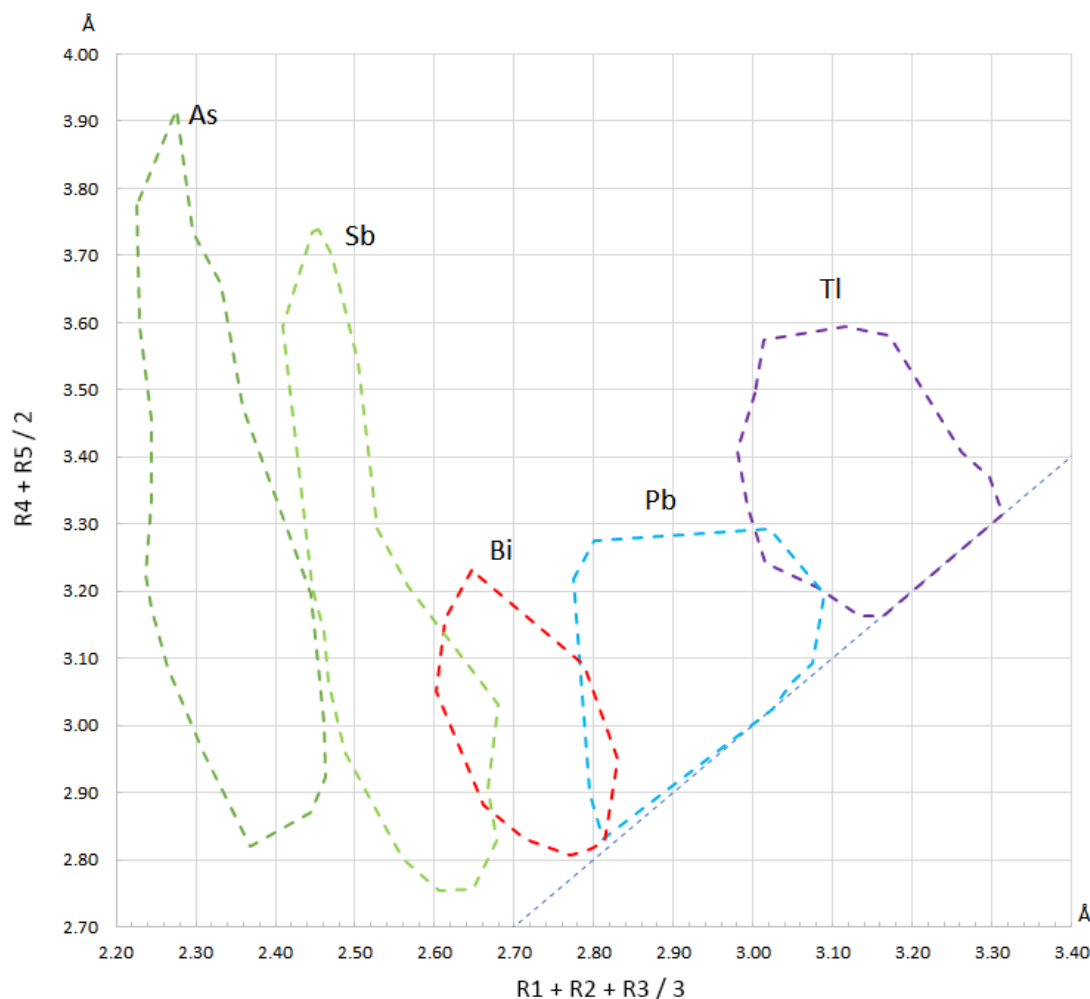


**Figure 23.** The Armbruster-Hummel diagram for discriminating As, Sb, Bi, Pb and Tl positions in sulfosalts. The diagonal corresponds to regular polyhedra where the five bond distances entailed by the method are equal. R1...R5 are bond lengths in ascending order.

The results of the 123/45 averages calculation are displayed at the push of the [Coordination geometry](#) button, with the [Detailed results](#) ☒ control, checked on. In this display context, the results may be saved in CSV format by choosing **Save as type** 'ECoN21 123-45 bond averages (\*.csv)' in the **Save As...** dialog. A double-click on the file in Explorer, will open it in MS Excel where it can be edited and transferred to the template sheet *OpposingBonds.xlsx* which comes packed with the main program.

## 10 Release notes

### Release 1.2

- CIF files generated by Jana2006, which may contain multiple occurrences of the `_atom_site_label` flag and which had led to inadvertent reading of atom labels, symbols, coordinates, multiplicities and occupancies, are now read correctly.
- An error occurring when certain pairs of atoms did not have the  $R_o$  and  $B$  parameters listed in the *bvsparm.CIF* file has been prevented.
- A navigation aid for very long outputs has been added.

### Release 1.3

- The name of the program was changed from ECoN to ECoN21 in order to avoid confusion with the actual parameter *ECoN* used in the calculation. The program logo was modified.
- The following calculations have been added:
  - BVS around ligands;
  - expected distances, based on BVS;
  - Global Instability Index (Brown, 2009)
  - a new Distortion Index based on bond valence sum (Brown, 2006)
- The reference file for  $R_o$  and  $B$  parameters has been updated to the latest version issued by IUCr (Brown, 2020).
- The atom coordinates table is no longer a source for reading multiplicities. These are calculated exclusively using the symmetry operators.
- Unicode characters such as 'Δ' can now be saved in the text output file.
- The notation of various parameters has been simplified.
- The Access Violation errors which occurred on exiting the program have been corrected.

### Release 1.4

- The program is capable of treating heteroligand structures, both in the cation- and the anion-centered descriptions.
- New visualization aids have been added to switch rapidly between the results obtained in the two descriptions.
- A novel iteration method has been developed to refine the charges in heteroligand structures.
- The program can solve structures with hydrogen bonds.

### Release 1.5

- The CHARDI2015 iteration method for heteroligand polyhedra has been incorporated as an alternative to the native ECoN21 method.
- An optional 'one-step' iteration has been included.
- The calculation of  $EDEV_X$  ([Equation 28](#)) has been introduced.

### Release 1.6

- The possibility to set the maximum coordination radius for each chemical type of bond has been added.

- While in the previous releases, the *BVS* calculation was discarded altogether when a single required pair of  $R_o$  and  $B$  was missing from the *bvsparm.cif* file, now the *BVS* is omitted only for polyhedra with missing parameters. However, the *MAPDs* for *BVS* and the global instability index are not calculated for such structures.
- Bond angles have been included in the connectivity calculation.
- The automatic saving of the results displayed in the output window, is now optional.
- The summary of the results can now be saved in *.csv* format for direct import into MS Excel.

#### Release 1.7

- Ligands located beyond the nearest neighboring central atom may now be excluded automatically from the coordination polyhedra.
- Coordination polyhedra based exclusively on non-zero-weight bonds, may now be preset.
- Optional manual setting of the coordination number for each polyhedron has been added.
- The calculation of various quantities deriving from the centroid of coordination has been included in the new **Coordination geometry** section of the program:
  - the coordinates of the centroid;
  - the components of the vector between the central atom and the centroid;
  - the displacement of the central atom from the centroid;
  - the radius and volume of the least-squares fitted 'circumsphere';
  - the linear and 'volume-based' eccentricity of the central atom;
  - the linear and 'volume-based' sphericity of the ligand distribution;
  - the volume of the coordination polyhedron;
  - the approximation of the ideal polyhedron of maximum volume inscribed in the least-squares fitted 'circumsphere';
  - the volume of the ideal polyhedron inscribable in the least-squares fitted 'circumsphere' and which has the maximum possible volume for that sphere;
  - the volume (external) distortion of the coordination polyhedron;
- A minimal dihedral angle for merging adjacent CP faces into a single, 'flat' one has been added to the **Calculation settings**.
- A list of interligand distances has been included in the **Coordination geometry** output.
- The program calculates the dihedral angles between each triangular face used in the calculation of the CP volume and its adjacent faces.
- Distances between central atoms and the nearest neighboring central atoms have also been introduced.
- The mean absolute percentage deviation of  $Q_A$  values for the ligands of each CP has been included in the calculation.
- Extra options for ending the iteration process in the CD calculation of heteroligand structures have been introduced.

#### Release 1.8

- An error produced by cations and anions sharing the same 'extra framework' positions in the crystal structure (*e.g.*,  $\text{Cs}^+$  and  $\text{H}_2\text{O}$ -linked  $\text{O}^{2-}$  in tunnel sites of cordierite) has been corrected.

- A seldom occurring error produced by the rounding of coordinates for generated atoms and corrupting the calculated multiplicities, has been corrected.
- An even less frequent error caused by missing parentheses around standard deviations in the CIF file has been fixed.
- An error occurring in the calculation of charge distribution, related to the connectivity of symmetry generated ligands, has been corrected.
- The program now identifies the 'in plane' and 'out of plane' bond pairs in the cation-centered description to be used in the Trömel diagram.
- The calculation of the 123/45 averages in preparation of Armbruster-Hummel diagram, has been introduced.
- A MS Excel template—*OpposingBonds.xlsx*—containing dedicated columns for data transfer, a diagram with bond-length ratio hyperbolae for Pb-, As-, Sb-, Bi- and Sn-S as well as the Armbruster-Hummel diagram, has been included in the program's package.
- Some calculations concerning the **Coordination Geometry** are now optional and can be set on and off in the **Calculation Settings** dialog.
- The calculation of volumes for coordination polyhedra in the shape of hexagonal (anti)prisms is now possible.



## 11 References

- ARMBRUSTER T., HUMMEL W. (1987) (Sb,Bi,Pb) ordering in sulfosalts: Crystal-structure refinement of a Bi-rich izoklakeite. *American Mineralogist* **72**: 821-831.
- BAUR W.H. (1974) The geometry of polyhedral distortions. Predictive relationships for the phosphate group. *Acta Crystallographica* **B30**: 1195–1215.
- BALIĆ-ŽUNIĆ T., VICKOVIĆ I. (1996) IVTON—Program for the calculation of geometrical aspects of crystal structures and some crystal chemical applications. *Journal of Applied Crystallography* **29**, 305–306.
- BERLEPSCH P., MAKOVICKY E., BALIĆ-ŽUNIĆ T. (2001a) Crystal chemistry of meneghinite homologues and related sulfosalts. *Neues Jahrbuch der Mineralogie, Monatshefte* **2001**, 115-135.
- BERLEPSCH P., MAKOVICKY E., BALIĆ-ŽUNIĆ T. (2001b): Crystal chemistry of sartorite homologues and related sulfosalts. *Neues Jahrbuch der Mineralogie, Abhandlungen* **176**, 45-66.
- BERLEPSCH P., ARMBRUSTER E., TOPA D. (2002): Structural and chemical variations in rathite,  $\text{Pb}_8\text{Pb}_{4-x}(\text{Te}_2\text{As}_2)_x(\text{Ag}_2\text{As}_2)\text{As}_{16}\text{S}_{40}$ : modulations of a parent structure. *Zeitschrift für Kristallographie* **217**, 581–590.
- BOSI F. (2014) Bond valence at mixed occupancy sites. I. Regular polyhedra. *Acta Crystallogr.* **B70**: 864–870.
- BRENNAN T.D., IBERS J.A. (1991) Lanthanum orthosilicate selenide,  $\text{La}_2\text{SeSiO}_4$ . *Acta Crystallographica* **C47**: 1062–1064.
- BRESE N.E., O'KEEFFE M. (1991) Bond–Valence Parameters for Solids. *Acta Crystallogr.* **B47**: 192–197.
- BROWN I.D. (2006) On measuring the size of distortions in coordination polyhedra. *Acta Crystallographica* **B62**: 692–694.
- BROWN I.D. (2009) Recent developments in methods and applications of the bond valence model. *Chemical Reviews* **109**: 6858–6919.
- BROWN I.D. (2020) Accumulated list of bond valence parameters. Available for download at: <https://www.iucr.org/resources/data/datasets/bond-valence-parameters>
- BROWN I.D., ALTERMATT D. (1985) Bond–valence parameters obtained from a systematic analysis of the Inorganic Crystal Structure Database. *Acta Crystallographica* **B41**: 244–247.
- ENGEL P., NOWACKI W. (1969) Die Kristallstruktur von Baumhauerit. *Zeitschrift für Kristallographie* **129**, 178–202.
- EON J–G., NESPOLO M. (2015) Charge distribution as a tool to investigate structural details. III. Extension to description in terms of anion-centred polyhedra, *Acta Crystallographica* **B71**: 34–47.
- EVAIN M., BINDI L., MENCHETTI S. (2006) Structure and phase transition of the Se-rich variety of antimonpearceite,  $[(\text{Ag,Cu})_6(\text{Sb,As})_2(\text{S,Se})_7][\text{Ag}_3\text{Cu}(\text{S,Se})_2\text{Se}_2]$ . *Acta Crystallographica* **B62**: 768–774.

- FERRARIS G. (2011) Inorganic and mineral crystals. In: Giacobbo C. (ed.) *Fundamentals of Crystallography*, 3<sup>rd</sup> Edition, Oxford University Press pp 512–591.
- GAGNÉ O.C., HAWTHORNE F.K. (2015) Comprehensive derivation of bond-valence parameters for ion pairs involving oxygen. *Acta Crystallogr.* **B71**: 562–578.
- HOPPE R., VOIGT S., GLAUM H., KISSEL J., MÜLLER H.P., BERNET K. (1989) A new route to charge distributions in ionic solids, *Journal of the Less-Common Metals* **156**: 105–122.
- HOPPE R. (1979) Effective coordination numbers (ECoN) and mean fictive ionic radii (MEFIR), *Zeitschrift für Kristallographie* **150**: 23–52.
- HUMMEL W., ARMBRUSTER T. (1987)  $\text{Ti}^+$ ,  $\text{Pb}^{2+}$ , and  $\text{Bi}^{3+}$  bonding and ordering in sulfides and sulfosalts. *Schweizerische mineralogische und petrographische Mitteilungen* **67/3**: 213–218.
- MAKOVICKY E., BALIĆ-ŽUNIĆ T. (1996) Determination of the Centroid or ‘the Best Centre’ of a Coordination Polyhedron. *Acta Crystallographica* **B52**, 78–81.
- MAKOVICKY E., BALIĆ-ŽUNIĆ T. (1998) New Measure of Distortion for Coordination Polyhedra. *Acta Crystallographica* **B54**, 766–773.
- MOMMA K., IZUMI F. (2011) VESTA 3 for three-dimensional visualization of crystal, volumetric and morphology data, *Journal of Applied Crystallography* **44**: 1272–1276.
- NAKASHIMA M., ARMBRUSTER T., IZUMINO Y., NAKASHIMA K. (2013) Crystal chemistry of a Cu isotype of makovickyite from the Obari mine, Yamagata Prefecture, Japan. *Neues Jahrbuch für Mineralogie, Abhandlungen* **191**, 75–81.
- NESPOLO M. (2016) Charge distribution as a tool to investigate structural details. IV. A new route to heteroligand polyhedra, *Acta Crystallographica* **B72**: 51–66.
- NESPOLO, M.; GUILLOT, B. (2016) CHARDI2015: charge distribution analysis of non-molecular structures. *Journal of Applied Crystallography* **49**: 317–321.
- NESPOLO M., FERRARIS G., OHASHI H. (1999) Charge distribution as a tool to investigate structural details: meaning and application to pyroxenes. *Acta Crystallographica* **B55**: 902–916.
- NESPOLO M., FERRARIS G., IVALDI G., HOPPE R. (2001) Charge distribution as a tool to investigate structural details. II. Extension to hydrogen bonds, distorted and hetero-ligand polyhedra. *Acta Crystallographica* **B57**: 652–664.
- PAULING L. (1929) The principles determining the structure of complex ionic crystals. *Journal of the American Chemical Society* **51**: 1010–1026.
- PETŘÍČEK V., DUŠEK M., PALATINUS L. (2006) Crystallographic Computing System JANA2006: General features, *Zeitschrift für Kristallographie* **229(5)**: 345–352.
- SEJKORA J., BERLEPSCH P., MAKOVICKY E., BALIĆ-ŽUNIĆ, T. (2001) Natural  $\text{SnGeS}_3$  from Radvanice near Trutnov (Czech Republic): Its Description, Crystal Structure Refinement and Solid Solution with  $\text{PbGeS}_3$ , *European Journal of Mineralogy* **13(4)**, 791–800. DOI:10.1127/0935-1221/2001/0013-0791

- TOPA D. (2001): Mineralogy, Crystal Structure and Crystal Chemistry of the Bismuthinite–Aikinite Series from Felbertal, Austria. Ph.D. thesis, Institute of Mineralogy, University of Salzburg, Austria.
- TOPA, D., MAKOVICKY, E., BALIĆ-ŽUNIĆ, T. (2003) Crystal structures and crystal chemistry of members of the cuprobismutite homologous series of sulfosalts. *Canadian Mineralogist* **41**: 1481–1501.
- TOPA D., MAKOVICKY E., DITTRICH H. (2010) The crystal structure of 7H : 12Q cannizzarite from Vulcano, Italy. *Canadian Mineralogist* **48(3)**: 483–495.
- TOPA D., KOLITSCH U. (2018) The Crystal Chemistry of Rathite Based on New Electron–Microprobe Data and Single–Crystal Structure Refinements: The Role of Thallium. *Minerals* **8**, 466.  
<https://doi.org/10.3390/min8100466>.
- TRÖMEL M. (1980) Empirische Beziehungen zur Sauerstoffkoordination um Antimon(III) und Tellur(IV) in Antimoniten und Telluriten. *Journal of Solid State Chemistry* **35**, 90-98.